

Magnetic field constraint for Majorana zero modes in a hybrid nanowireGuo-Jian Qiao (乔国健)¹, Sheng-Wen Li (李圣文)^{2,*} and C. P. Sun (孙昌璞)^{1,3,†}¹Beijing Computational Science Research Center, Beijing 100193, China²Center for Quantum Technology Research, and Key Laboratory of Advanced Optoelectronic Quantum Architecture and Measurements, School of Physics, Beijing Institute of Technology, Beijing 100081, People's Republic of China³Graduate School of China Academy of Engineering Physics, Beijing 100193, China

(Received 22 January 2022; revised 21 July 2022; accepted 20 September 2022; published 28 September 2022)

The hybrid semiconductor-superconductor nanowire is expected to serve as an experimental platform to support Majorana zero modes. By rederiving its effective Kitaev model with spins, we discover a topological phase diagram, which assigns a more precise constraint on the magnetic field strength for the emergence of Majorana zero modes. We find that the effective pairing strength dressed by the proximity effect exhibits a significant dependence on the magnetic field, and thus the topological phase region is refined into a closed triangle in the phase diagram with chemical potential vs Zeeman energy (which is obviously different from the open hyperbolic region known before). This prediction is confirmed again by an exact calculation of quantum transport, where the zero bias peak of $2e^2/h$ in the differential conductance spectrum, as the necessary evidence for the Majorana zero modes, disappears when the magnetic field grows too strong. Therefore, the hybrid nanowire system does not support Majorana zero modes under a too strong magnetic field. For illustrations with practical hybrid systems, in the InSb nanowire coupled to NbTiN, the accessible magnetic field range is around 0.1–1.5 T; when coupled to an aluminum shell, the accessible magnetic field range should be smaller than 0.12 T. Our predictions are essential to significantly narrow down the range of magnetic fields for further searching Majorana zero modes in experiments.

DOI: [10.1103/PhysRevB.106.104517](https://doi.org/10.1103/PhysRevB.106.104517)**I. INTRODUCTION**

Recent experiments for Majorana zero modes (MZMs) have attracted extensive attentions [1–7] due to their fractional statistics and potential applications in quantum computation [1,8,9]. In particular, the possible signature for MZMs has been shown in hybrid semiconductor-superconductor (HSS) systems [10,11], where a semiconductor nanowire with appreciable spin-orbit coupling is in contact with an *s*-wave superconductor (SC) providing the SC proximity effect. In transport experiments, the existence of MZMs would result in a zero bias peak (ZBP) in the differential conductance spectrum, and the height of the ZBP should be $2e^2/h$ in the ideal case at zero temperature [12–14].

However, most of the current ZBP detections for MZMs do not reach the ideal height of $2e^2/h$ but are lower [10,11,15,16]. As a result, such a ZBP signature alone cannot sufficiently confirm the existence of MZMs as the unique reason apart from other possible physical effects, such as Andreev bound states [7,17–19], and the Kondo effect [20,21]. To help narrow down the searching range in experiments, a more precise phase diagram for different parameter regimes is urgently needed to find the MZMs, for example, what is the allowed magnetic field range where the MZMs could exist.

In previous investigations, the SC proximity effect was assumed to be an *s*-wave pairing in the nanowire with the

pairing strength, which is approximated as a constant [2,22–26], and this is consistent with the result from the Bogoliubov–de Gennes equation projected into the low energy band [5,6,27–32]. It follows from this crude approximation that the topological region bearing MZMs fills up the whole upper half of a hyperbolic curve in the μ - B diagram (μ , B are the chemical potential and Zeeman splitting of the nanowire, respectively). Namely, these approximated results indicate MZMs exist no matter how strong the magnetic field grows. In this paper, however, we find that such a conclusion is not as solid as has been taken for granted, and MZMs emerge only when the magnetic field lies within a modest regime.

First, we utilize the Fröhlich-Nakajima (Schrieffer-Wolff) transformation to obtain an effective Hamiltonian for the nanowire, which encloses the SC proximity effect and then gives an effective Kitaev model in the HSS nanowire [33–35]. It turns out the effective pairing strength exhibits significant dependence on the strong magnetic field when the higher-order effect of the magnetic field is considered. As a result, the topological region bearing MZMs becomes a closed triangle in the μ - B diagram compared with the hyperbolic curve known before. Namely, when the magnetic field is too strong, the system becomes nontopological, and MZMs disappear; when the magnetic field is weak, this triangle region reduces to the previous hyperbolic curve. It is predicted from this phase diagram that the MZMs only emerge when the magnetic field strength lies within a modest regime. For the current experiments with InSb-NbTiN and InSb-Al, the magnetic field ranges supporting MZMs are 0.1–1.5 T and 0.012–0.12 T,

*lishengwen@bit.edu.cn

†suncp@giscaep.ac.cn

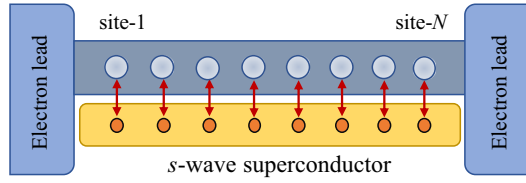


FIG. 1. Setup of the hybrid nanowire: The semiconductor nanowire is in contact with surface of the s -wave SC through tunneling. Through virtual exchanges of the quasiexcitations in the SC, this proximity effect induces an effective pairing among the electrons in the nanowire. In the experiment of quantum transport to probe Majorana zero modes, the hybrid system is connected to the electron leads.

respectively, the latter of which is outside the range used in some current experiments.

To confirm the above prediction based on the effective theory, we further make an exact calculation on the differential conductance in the transport measurement of the HSS nanowire by a quantum Langevin equation [36–40]. When the magnetic field increases from zero, a ZBP with $2e^2/h$ appears at a certain field strength, stays for a while, and then disappears at a higher strength, which is consistent with the conclusion from the effective Hamiltonian. This confirms that MZMs do not exist in the hybrid nanowire when the magnetic field is too strong.

II. EFFECTIVE KITAIEV MODEL IN LOW ENERGY SCALE

In this HSS system (see Fig. 1), the semiconductor nanowire is described by the Hamiltonian [3]

$$\hat{H}_w = \int dx \hat{\psi}^\dagger(x) \left[-\frac{\partial_x^2}{2m_w} - \mu - i\alpha\sigma^y\partial_x + B\sigma^z \right] \hat{\psi}(x), \quad (1)$$

where $\hat{\psi}(x) := [\hat{\psi}_\uparrow(x), \hat{\psi}_\downarrow(x)]^T$, and $\sigma^{y,z}$ are the Pauli matrices. Here \uparrow, \downarrow indicate the electron spins, α is the spin-orbit coupling strength, m_w is the effective mass, μ is the chemical potential of the nanowire, and B is the Zeeman splitting from the external magnetic field, respectively.

The semiconductor nanowire is placed in contact with an s -wave SC providing the SC proximity effect, which is described by the BCS Hamiltonian

$$\hat{H}_{sc} = \sum_{\mathbf{k}} \epsilon_{\mathbf{k}}^{sc} (\hat{c}_{\mathbf{k}\uparrow}^\dagger \hat{c}_{\mathbf{k}\uparrow} - \hat{c}_{-\mathbf{k}\downarrow} \hat{c}_{-\mathbf{k}\downarrow}^\dagger) + \Delta_s (\hat{c}_{\mathbf{k}\uparrow}^\dagger \hat{c}_{-\mathbf{k}\downarrow}^\dagger + \text{H.c.}), \quad (2)$$

with $\epsilon_{\mathbf{k}}^{sc} \equiv \mathbf{k}^2/2m_{sc} - \mu_{sc}$. The whole nanowire is contacted with the surface of the s -wave SC through the tunneling term

$$\hat{H}_{w-sc} = -J_s \sum_{s=\uparrow,\downarrow} \int dx [\hat{\psi}_s^\dagger(x) \hat{c}_s(x, 0, 0) + \text{H.c.}], \quad (3)$$

where J_s is the tunneling strength, and $\hat{c}_{\mathbf{k}s}$ and $\hat{c}_s(\mathbf{x})$ are the Fourier images of each other. The tunneling coupling induces an effective pairing among the electrons in the nanowire and this proximity effect is caused by the virtual exchanges of the quasiexcitations in the SC.

To describe the above mentioned virtual progress governed by the total Hamiltonian $\hat{\mathcal{H}} \equiv \hat{H}_w + \hat{H}_{sc} + \hat{H}_{w-sc}$, we apply the Fröhlich-Nakajima (Schrieffer-Wolff) transformation to

eliminate the degrees of freedom of the s -wave SC [33–35]. When the coupling between the nanowire and the s -wave SC is weak enough, the effective Hamiltonian for the nanowire is obtained as (see Appendix A)

$$\begin{aligned} \hat{H}_{\text{eff}} = & \int \frac{dk}{2\pi} \{ (\tilde{\epsilon}_{w,k} - \tilde{\mu}_k) [\hat{\phi}_\uparrow^\dagger(k) \hat{\phi}_\uparrow(k) + \hat{\phi}_\downarrow^\dagger(k) \hat{\phi}_\downarrow(k)] \\ & + i\tilde{\alpha}_k k [\hat{\phi}_\downarrow^\dagger(k) \hat{\phi}_\uparrow(k) - \text{H.c.}] \\ & + \tilde{B}_k [\hat{\phi}_\uparrow^\dagger(k) \hat{\phi}_\uparrow(k) - \hat{\phi}_\downarrow^\dagger(k) \hat{\phi}_\downarrow(k)] \\ & + \tilde{\Delta}_k [\hat{\phi}_\uparrow^\dagger(k) \hat{\phi}_\downarrow^\dagger(-k) + \text{H.c.}] \}. \end{aligned} \quad (4)$$

Here $\hat{\phi}_s(k)$ is the Fourier transform of $\hat{\psi}_s(x)$. $\tilde{\Delta}_k$ is the effective pairing strength induced by the SC proximity effect, and $\tilde{\epsilon}_{w,k}$, $\tilde{\mu}_k$, $\tilde{\alpha}_k$, and \tilde{B}_k are the corrected kinetic energy ($\epsilon_{w,k} \equiv k^2/2m_w$), chemical potential, spin-orbit coupling, and Zeeman splitting of the nanowire, respectively, i.e.,

$$\begin{aligned} \tilde{\Delta}_k &= \Upsilon_s \left[1 - \frac{\alpha^2 k^2 + B^2}{\Delta_s^2} \right]^{-\frac{1}{2}}, \\ \frac{\tilde{\epsilon}_{w,k}}{\epsilon_{w,k}} = \frac{\tilde{\mu}_k}{\mu} = \frac{\tilde{\alpha}_k}{\alpha} = \frac{\tilde{B}_k}{B} &= 1 - \frac{\tilde{\Delta}_k}{\Delta_s}. \end{aligned} \quad (5)$$

Here $\Upsilon_s := J_s^2 \rho_s$ describes the coupling strength between the nanowire and the s -wave SC, with ρ_s as the density of states from the s -wave SC, and approximately Υ_s is a constant.

Notice that here the dependence on the magnetic field B is well kept in the above corrected parameters (5). Usually, the induced s -wave pairing is regarded as a constant in previous studies, and the high-order dependencies on B/Δ_s in Eq. (5) are ignored. However, in the following, we show that such high-order dependencies are essential when studying the phase diagram in the strong field regime.

Under the open boundary condition, the effective Hamiltonian (4) has two edge modes localized at the two ends of the nanowire, whose mode energies are zero, and they are just the MZMs. It can be proved that the existence condition for the MZMs is given by the critical condition $[\tilde{B}_k^2 - \tilde{\mu}_k^2 - \tilde{\Delta}_k^2]_{k=0} = 0$ (see Appendix B), which determines the topological phase region [3,41]. It turns out this topological region bearing MZMs appears as a closed triangle in the μ - B phase diagram (Fig. 2). For a fixed chemical potential μ , the MZMs could emerge only if the magnetic field strength properly lies inside the triangle range. It is worth emphasizing that the magnetic field range determined by the closed phase diagram is much smaller than the critical magnetic field of the s -wave superconductor (respectively $B_c \sim 10$ T and $B_{\perp,c} \sim 0.1$ T, $B_{\parallel,c} \sim 1$ T for NbTiN and Al [4,42]). However, the s -wave SC gap Δ_s would also decrease with the increase of the magnetic field. This effect is not considered, and Δ_s is treated as a constant independent of the magnetic field. If this effect is considered, the topological region in Fig. 2 would be smaller. Thus, when the magnetic field strength exceeds the range of the magnetic field determined by refined phase region, the effective Hamiltonian (4) of the hybrid nanowire does not support the existence of the MZMs.

For the weak field situation ($B \ll \Delta_s$), in the low energy regime ($k \simeq 0$), the induced pairing strength can be approximated as a constant $\tilde{\Delta}_k \simeq \Upsilon_s$ [see Eq. (5)]. Correspondingly,

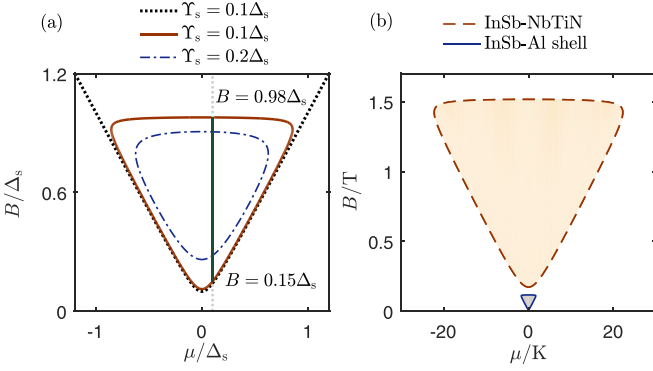


FIG. 2. (a) The topological phase diagram for HSS nanowire given by the effective Hamiltonian (4) scaled by Δ_s . The topological phase region bearing MZMs is a closed triangle. The dotted black line is given by the approximated topological criterion $B^2 - \mu^2 = \Upsilon_s^2$ [3,41]. The vertical line is $\mu = 0.1 \Delta_s$, and the valid range for the magnetic field is $B \sim 0.15\text{--}0.98 \Delta_s$. (b) The rescaled phased diagram. For InSb nanowire (Landé factor $g \simeq 50$) coupled to NbTiN as the s -wave SC ($\Delta_s \simeq 26$ K [10]), the valid topological phase lies in the yellow region, with the magnetic field range $B \sim 0.15\text{--}1.5$ T; for InSb nanowire coupled to aluminum shell ($\Delta_s \simeq 2$ K [4,43]), the valid topological phase lies in the smaller gray region, with the magnetic field range around $0.012\text{--}0.12$ T, where MZMs could exist.

the above topological phase condition is reduced as $B^2 - \mu^2 = \Upsilon_s^2 / (1 - \Upsilon_s / \Delta_s)^2 \simeq \Upsilon_s^2$, which just returns the hyperbolic curve extensively studied in previous literatures [3,41]. Indeed, the bottom part of the close triangle region and the hyperbolic curve agree well with each other (Fig. 2), which is consistent with the fact that the hyperbolic curve comes from an effective theory in the low energy regime.

To have a more clear understanding of the above observations, we study the above effective Hamiltonian in a new representation [by diagonalizing the first three bracket terms of (4)],

$$\begin{aligned} \hat{H}_{\text{eff}} = & \int \frac{dk}{2\pi} \{ \tilde{\varepsilon}_{k+} \hat{\varphi}_+^\dagger(k) \hat{\varphi}_+(k) + \tilde{\varepsilon}_{k-} \hat{\varphi}_-^\dagger(k) \hat{\varphi}_-(k) \\ & + \frac{1}{2} \tilde{\Delta}_k^{(p)} [\hat{\varphi}_+^\dagger(k) \hat{\varphi}_+^\dagger(-k) + \hat{\varphi}_-^\dagger(k) \hat{\varphi}_-^\dagger(-k) + \text{H.c.}] \\ & + \tilde{\Delta}_k^{(s)} [\hat{\varphi}_+^\dagger(k) \hat{\varphi}_-^\dagger(-k) + \text{H.c.}] \}, \end{aligned} \quad (6)$$

which appears as an effective Kitaev model with spins [1,44]. Here $\tilde{\varepsilon}_{k\pm} = \tilde{\varepsilon}_{w,k} - \tilde{\mu}_k \pm \sqrt{\tilde{B}_k^2 + \tilde{\alpha}_k^2 k^2}$, and

$$\begin{aligned} \tilde{\Delta}_k^{(p)} & := \frac{\alpha k \tilde{\Delta}_k}{\sqrt{B^2 + \alpha^2 k^2}}, \quad \tilde{\Delta}_k^{(s)} := \frac{B \tilde{\Delta}_k}{\sqrt{B^2 + \alpha^2 k^2}}, \\ \begin{bmatrix} \hat{\varphi}_+(k) \\ \hat{\varphi}_-(k) \end{bmatrix} & := \begin{bmatrix} \cos \vartheta_k & i \sin \vartheta_k \\ -i \sin \vartheta_k & \cos \vartheta_k \end{bmatrix} \begin{bmatrix} \hat{\varphi}_\uparrow(k) \\ \hat{\varphi}_\downarrow(k) \end{bmatrix}, \end{aligned} \quad (7)$$

with $\tan 2\vartheta_k = \tilde{\alpha}_k k / \tilde{B}_k = \alpha k / B$.

In the above representation, $\tilde{\Delta}_k^{(s)}$ and $\tilde{\Delta}_k^{(p)}$ are effectively regarded as the s -wave and p -wave pairing strength, respectively. With the increase of the magnetic field B , the p -wave pairing $\tilde{\Delta}_k^{(p)}$ becomes weaker and weaker, while relatively the s -wave pairing $\tilde{\Delta}_k^{(s)}$ becomes more dominant. Thus when the magnetic field is too strong, the nanowire system enters

the nontopological phase region, and the MZMs would disappear. Indeed, the disappearance of ZBP in the strong magnetic field was claimed in some of the current experiments [10,11], which is well explained by our result.

III. THE HYBRID NANOWIRE OF QUANTUM TRANSPORT

To confirm the above observations from the effective Hamiltonian, we carry out an exact calculation of the transport behavior for the hybrid nanowire. To this end, the above continuous Hamiltonian (1) is first discretized into an N -site system as [26,45–47]

$$\begin{aligned} \hat{H}_w = & \sum_{n,s} -\frac{J}{2} (\hat{d}_{n,s}^\dagger \hat{d}_{n+1,s} + \hat{d}_{n+1,s}^\dagger \hat{d}_{n,s}) - (\mu - J) \hat{d}_{n,s}^\dagger \hat{d}_{n,s} \\ & + \sum_n \frac{\alpha_R}{2} (\hat{d}_{n,\downarrow}^\dagger \hat{d}_{n+1,\uparrow} - \hat{d}_{n,\uparrow}^\dagger \hat{d}_{n+1,\downarrow} + \text{H.c.}) \\ & + \sum_n B (\hat{d}_{n,\uparrow}^\dagger \hat{d}_{n,\uparrow} - \hat{d}_{n,\downarrow}^\dagger \hat{d}_{n,\downarrow}). \end{aligned} \quad (8)$$

Correspondingly, the tunneling term (3) between the nanowire and the s -wave SC becomes $\hat{H}_{w\text{-sc}} = -\sum_{n,\mathbf{k}s} (J_{n,\mathbf{k}s} \hat{d}_{n,s}^\dagger \hat{c}_{\mathbf{k}s} + \text{H.c.})$, with the tunneling strength $|J_{m,\mathbf{k}s}| = |J_{n,\mathbf{k}s}'| := J_{\mathbf{k}}$ for $m \neq n, s \neq s'$. We consider two electron leads are in contact with the two ends of the nanowire (the site number $x = 1, N$), which are described by the free electron gas model of metal $\hat{H}_{e-x} = \sum_{\mathbf{k}s} \varepsilon_{x,\mathbf{k}} \hat{b}_{x,\mathbf{k}s}^\dagger \hat{b}_{x,\mathbf{k}s}$. The kinetic of the free electron with respect to the chemical μ_x is $\varepsilon_{x,\mathbf{k}} = k^2 / 2m - \mu_x$. The tunneling interaction between the nanowire and lead x is $\hat{H}_{w-x} = -\sum_{\mathbf{k}s} (g_{x,\mathbf{k}} \hat{d}_{n,s}^\dagger \hat{b}_{x,\mathbf{k}s} + \text{H.c.})$.

The semiconductor nanowire is in contact with an s -wave SC providing the SC proximity effect, which is described by the BCS Hamiltonian with $\epsilon_{\mathbf{k}}^{\text{sc}} \equiv k^2 / 2m_{\text{sc}} - \mu_{\text{sc}}$ and the constant s -wave pairing strength Δ_s [see Eq. (2)]. All the N nanowire sites are contacted with the s -wave SC through the tunneling interaction, which is described by $\hat{H}_{w\text{-sc}} = -\sum_{n,\mathbf{k}s} (J_{n,\mathbf{k}} \hat{d}_{n,s}^\dagger \hat{c}_{\mathbf{k}s} + \text{H.c.})$, with $J_{n,\mathbf{k}}$ as the tunneling strength between site n and the s -wave SC, and they have the same amplitude $|J_{n,\mathbf{k}}| = |J_{m,\mathbf{k}}| := J_{\mathbf{k}}$ for different sites $m \neq n$.

Notice that, similar to the two electron leads, indeed the s -wave SC is also regarded as the third fermionic bath interacting with the nanowire. Here we use the quantum Langevin equation to study the transport current through the nanowire [36–40], which is derived by combining the Heisenberg equations of \hat{d}_{ns} (nanowire), $\hat{c}_{\mathbf{k}s}$ (s -wave SC), and $\hat{b}_{x,\mathbf{k}s}$ (electron leads), that is (see Appendix C),

$$\partial_t \hat{\mathbf{d}} = -i \mathbf{H}_w \cdot \hat{\mathbf{d}} - \int_0^t d\tau \mathbf{D}(t - \tau) \cdot \hat{\mathbf{d}}(\tau) + i \hat{\xi}_{\text{sc}} + i \hat{\xi}_e. \quad (9)$$

Here $\hat{\mathbf{d}}(t) := (\hat{d}_1, \dots, \hat{d}_N)^T$ is a $4N$ -vector form with N blocks $\hat{\mathbf{d}}_n := (\hat{d}_{n\uparrow}, \hat{d}_{n\downarrow}, \hat{d}_{n\uparrow}^\dagger, \hat{d}_{n\downarrow}^\dagger)^T$ and the nanowire Hamiltonian $\hat{H}_w \equiv \frac{1}{2} \hat{\mathbf{d}}^\dagger \cdot \mathbf{H}_w \cdot \hat{\mathbf{d}}$ is rewritten with a $4N \times 4N$ matrix \mathbf{H}_w . The dissipation kernel $\mathbf{D}(t) \equiv \mathbf{D}_e(t) + \mathbf{D}_{\text{sc}}(t)$ contains the contributions from both the two electron leads and the s -wave SC, and $\hat{\xi}_e(t)$ and $\hat{\xi}_{\text{sc}}(t)$ are the corresponding random forces, respectively.

The Langevin equation (9) of $\hat{\mathbf{d}}(t)$ is exactly solved in the Fourier space as $\hat{\mathbf{d}}(\omega) = \mathbf{G}(\omega) \cdot [\hat{\mathbf{d}}_{(t=0)} + i\tilde{\xi}_{\text{sc}}(\omega) + i\tilde{\xi}_e(\omega)]$, where $[\mathbf{G}(\omega)]_{4N \times 4N}$ is the Green function of the nanowire,

$$\begin{aligned} \mathbf{G}(\omega) &= i[\omega^+ - \mathbf{H}_w + i\tilde{\mathbf{D}}_{\text{sc}}(\omega) + i\tilde{\mathbf{D}}_e(\omega)]^{-1} \\ &\equiv i \left\{ \omega^+ - \mathbf{H}_w - \tilde{\mathbf{V}}_s(\omega) + \frac{i}{2} [\tilde{\mathbf{\Gamma}}_s(\omega) + \tilde{\mathbf{\Gamma}}_e(\omega)] \right\}^{-1}, \end{aligned} \quad (10)$$

with $\omega^+ \equiv \omega + i\epsilon$ (ϵ is infinitesimal). Here $\tilde{\mathbf{D}}_{\text{sc}}(\omega) \equiv \tilde{\mathbf{\Gamma}}_s(\omega)/2 + i\tilde{\mathbf{V}}_s(\omega)$ is the Fourier image of the dissipation kernel $\mathbf{D}_{\text{sc}}(t)$ from the s -wave SC, where the ‘‘real part’’ $\tilde{\mathbf{\Gamma}}_s(\omega)$ leads to dissipation, and the ‘‘imaginary part’’ $\tilde{\mathbf{V}}_s(\omega)$ provides an effective interaction for the nanowire Hamiltonian.

Specifically, $\tilde{\mathbf{D}}_{\text{sc}}(\omega) := \text{diag}\{\tilde{\mathbf{D}}_s, \dots, \tilde{\mathbf{D}}_s\}$ is a block-diagonal matrix, with blocks $\tilde{\mathbf{D}}_s(\omega) := \tilde{\mathbf{\Gamma}}_s(\omega)/2 + i\tilde{\mathbf{V}}_s(\omega)$, where $\tilde{\mathbf{\Gamma}}_s(\omega) := \tilde{\mathbf{\Gamma}}_s^+(\omega) + \tilde{\mathbf{\Gamma}}_s^-(\omega)$ and

$$\begin{aligned} \tilde{\mathbf{V}}_s(\omega) &:= -\frac{\Theta(\Delta_s - |\omega|)\Upsilon_s}{\sqrt{\Delta_s^2 - \omega^2}} \Sigma(\omega), \\ \tilde{\mathbf{\Gamma}}_s^\pm(\omega) &:= \pm \frac{2\Theta(\pm\omega - \Delta_s)\Upsilon_s}{\sqrt{\omega^2 - \Delta_s^2}} \Sigma(\omega), \\ \Sigma(\omega) &:= \begin{bmatrix} \omega & 0 & 0 & -\Delta_s \\ 0 & \omega & \Delta_s & 0 \\ 0 & \Delta_s & \omega & 0 \\ -\Delta_s & 0 & 0 & \omega \end{bmatrix}. \end{aligned} \quad (11)$$

Here $\Upsilon_s(\omega) := \pi \sum_{\mathbf{k}} |\mathbf{J}_{\mathbf{k}}|^2 \delta(\omega - \epsilon_{\mathbf{k}}^{\text{sc}}) \rightarrow \pi |\mathbf{J}_s(\omega)|^2 \rho_s(\omega)$ is introduced as the spectral density of the coupling with the s -wave SC, which is approximated as a constant coupling strength $\Upsilon_s(\omega) \simeq \Upsilon_s$.

The dissipation kernels of the two electron leads also give $\tilde{\mathbf{D}}_e(\omega) \equiv \tilde{\mathbf{\Gamma}}_e(\omega)/2 + i\tilde{\mathbf{V}}_e(\omega)$, while $\tilde{\mathbf{V}}_e(\omega) \simeq 0$ in the usual transport experiments, only with $\tilde{\mathbf{\Gamma}}_e(\omega) := \mathbf{\Gamma}_1 + \mathbf{\Gamma}_N$ left providing dissipation to the system. Here $\mathbf{\Gamma}_1 := \text{diag}\{\Gamma_1, \mathbf{0}, \dots, \mathbf{0}\}$ and $\mathbf{\Gamma}_N := \text{diag}\{\mathbf{0}, \dots, \mathbf{0}, \Gamma_N\}$ are the dissipation matrices from the two electron leads respectively, where $\Gamma_x := \Upsilon_x \mathbf{1}_{4 \times 4}$ ($x = 1, N$), and Υ_x indicates the coupling strength with lead- x , defined from the coupling spectral density $\Upsilon_x(\omega) := 2\pi \sum_{\mathbf{k}} |\mathbf{g}_{x,\mathbf{k}}|^2 \delta(\omega - \epsilon_{x,\mathbf{k}}) \simeq \Upsilon_x$.

It is worth noting that, without deriving the effective Hamiltonian *in priori* with any approximations, the SC proximity effect is naturally presented as off-diagonal elements of $\tilde{\mathbf{V}}_s(\omega)$ in the dynamical propagator (10), which measures the on-site s -wave pairing for the nanowire [7,28,44,45]. Moreover, a Heaviside function appears in both $\tilde{\mathbf{V}}_s(\omega)$ and $\tilde{\mathbf{\Gamma}}_s(\omega)$, indicating a complementary effect of the SC proximity: when the system energy scale lies within the s -wave gap $|\omega| < \Delta_s$, the s -wave SC just provides the effective pairing interaction without any dissipation; in contrast, outside the gap $|\omega| > \Delta_s$, the SC proximity does not give the effective pairing, but only brings in the dissipation effect similarly as the normal leads.

IV. TRANSPORT SIGNATURE

To study the transport current, we consider the initial states of the three baths (the two normal leads, and the s -wave

SC) in the Fermi-Dirac distributions at zero temperature. The chemical potentials of the electron lead N is set as $\mu_N = 0$, while the lead 1 is $\mu_1 = eV$ with V the bias voltage.

The electric current flowing from lead 1 to the nanowire is obtained from the changing rate of the total electron number in lead 1, i.e., $\hat{I}_1(t) := -e \partial_t \sum_{\mathbf{k}s} \langle \hat{b}_{1,\mathbf{k}s}^\dagger \hat{b}_{1,\mathbf{k}s} \rangle$. After a long enough time relaxation $t \rightarrow \infty$, by the solution (10) of the above quantum Langevin equation in the Fourier space, a steady current is achieved without any approximation. Furthermore, the exact differential conductance $\sigma \equiv dI_1/dV$ is obtained as (see Appendix E)

$$\begin{aligned} \sigma &= \frac{e^2}{h} \{ \text{tr}[\mathbf{G}^\dagger \mathbf{\Gamma}_1^+ \mathbf{G} \mathbf{\Gamma}_N]_{(eV)} + \text{tr}[\mathbf{G}^\dagger \mathbf{\Gamma}_1^+ \mathbf{G} \tilde{\mathbf{\Gamma}}_s]_{(eV)} \\ &\quad + \text{tr}[\mathbf{G}^\dagger \mathbf{\Gamma}_1^+ \mathbf{G} \mathbf{\Gamma}_1^-]_{(eV)} + \text{tr}[\mathbf{G}^\dagger \mathbf{\Gamma}_1^+ \mathbf{G} \mathbf{\Gamma}_1^-]_{(-eV)} \}. \end{aligned} \quad (12)$$

Here the dissipation matrices $\mathbf{\Gamma}_{1,N}^\pm$ are given by $\mathbf{\Gamma}_1^\pm := \text{diag}\{\Gamma_1^\pm, \mathbf{0}, \dots, \mathbf{0}\}$, and $\mathbf{\Gamma}_N^\pm := \text{diag}\{\mathbf{0}, \dots, \mathbf{0}, \Gamma_N^\pm\}$, with the 4×4 blocks $\Gamma_x^+ := \Upsilon_x \text{diag}\{1, 1, 0, 0\}$, and $\Gamma_x^- := \Upsilon_x \text{diag}\{0, 0, 1, 1\}$. Similarly, the dissipation matrix $\tilde{\mathbf{\Gamma}}_s(\omega)$ also has been obtained by dissipation kernel of SC in Eq. (11).

The first two terms in Eq. (12) come from the electron exchanges among lead 1 to lead N and the s -wave SC, respectively; the last two terms indicate the contribution from the Andreev reflection between lead 1 and the nanowire, which gives the ZBP of $2e^2/h$ as the necessary signature for the emergence of MZMs at zero temperature [12,13,38,40]. Up to now, no other approximations are made except the form of the coupling spectral density, thus the obtained result is sufficiently accurate even for the situations when the coupling strength or the magnetic field is quite strong.

The corresponding numerical results under different physical conditions are illustrated in Fig. 3. It is shown that a ZBP with height $2e^2/h$ appears in the conductance spectrum when the magnetic field B lies in a continuous regime of modest strength. The ZBP disappears when the magnetic field strength is too weak or too strong, thus, it is confirmed that the MZMs do not exist in these regimes. The similar phenomenon for the refined magnetic field constraint in the phase diagram of the multiband nanowire models has also been discussed based on the low-energy effective Hamiltonian [48]. The trend of changing ZBP signature with the magnetic field is fitted with the observed result in experiment [10,11,49].

It is especially worth noting that under certain conditions the ZBP could be even higher than $2e^2/h$ [see Figs. 3(e) and 3(f)] which may be caused by the bulk states or subgap states in the induced gap of the nanowire. When the more bulk states are involved in electron transport, or subgap states approach zero energy with the magnetic increase, the differential conductance σ will increase continuously and even more than $2e^2/h$. At finite temperatures, such a ZBP would be as low as $2e^2/h$ and thus might be confused with the signature from MZMs. Therefore, it should be emphasized that the ZBP of $2e^2/h$ is the necessary but not sufficient condition for the MZMs and may represent MZMs only when the range of chemical potential and the magnetic field strength is within the topological phase region determined by the effective Kitaev Hamiltonian of the hybrid nanowire system.

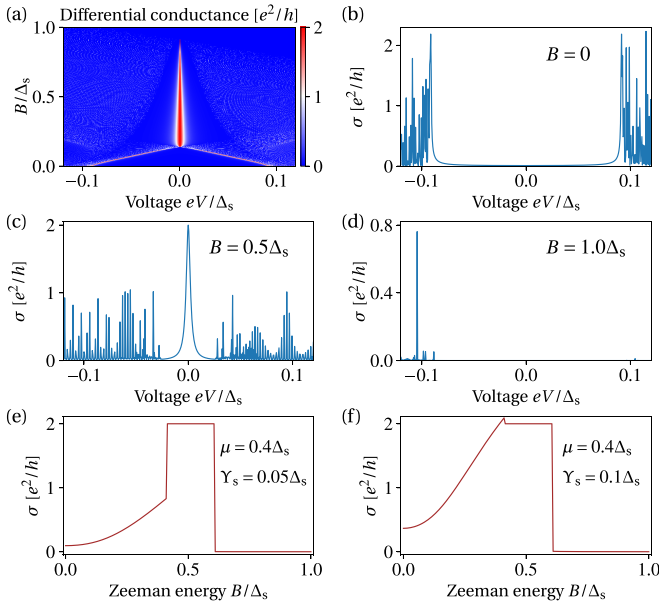


FIG. 3. (a) The differential conductance $\sigma = dI_1/dV$ depending on the bias voltage and the magnetic field (site number $N = 500$). Here Δ_s is set as the energy unit, and the other parameters are set as $\mu = 0.1\Delta_s$, $\alpha_R = 0.15\Delta_s$, $J = 0.5\Delta_s$, $\Upsilon_s = 0.1\Delta_s$, $\Upsilon_1 = \Upsilon_N = 0.025\Delta_s$. (b)–(d) The differential conductance depending on the bias voltage, when the Zeeman energies are fixed as $B/\Delta_s = 0, 0.5, 1.0$, respectively. (e) and (f) The differential conductance at $V = 0$ depends on the magnetic field B . Under certain parameters, the ZBP could be higher than $2e^2/h$, which indicates this is not from the MZMs.

V. SUMMARY

By examining the the low-energy effective model for the hybrid system with the semiconductor nanowire in proximity to the s -wave superconductor, we obtain a refined topolog-

ical phase diagram where the Majorana zero modes (MZMs) could exist but over a confined parameter region. The affirmed topological phase region bearing MZMs appears as a closed triangle in the μ - B phase diagram, in comparison with the open hyperbolic region known before. These predictions are also confirmed by an exact calculation of the quantum transport based on the quantum Langevin equation: in the transport spectrum, the zero bias peak with $2e^2/h$, as the necessary signature for MZMs, disappears when the magnetic field grows too strong. Therefore, we claim that the hybrid nanowire does not support MZMs under a strong magnetic field.

To search for MZMs in this hybrid nanowire system, we suggest that the magnetic field strength be properly set within a modest range according to our phase diagram. For the electron-doped InSb nanowire coupled to NbTiN ($\Delta_s \simeq 26$ K), the chemical potential is around $\mu \sim 0$ –10 K, the spin-orbit energy is around $2m_w\alpha^2 \sim 1$ –3 K [4,10,11,24,42,43,50–51], and the above results show that the proper range for the magnetic field is around $B \sim 0.1$ –1.5 T where MZMs could exist. For InSb nanowire coupled to an aluminum shell ($\Delta_s \simeq 2$ K) [4,43], the convincing range for the magnetic field is no greater than 0.12 T. However, some of the recent experiments claim the emergence of MZMs when the magnetic field strength exceeds much beyond the validity range we obtained in this paper. It is believed that our current theoretical study will help narrow down the range of magnetic fields for further searching Majorana zero modes in experiments.

ACKNOWLEDGMENTS

The authors very much appreciate the helpful discussions with Y. Chen in CAEP, X. Dai in HKUST, Y.-N. Fang in Yunnan University, R.-B. Liu in CUHK, X.-J. Liu in Peking University, and Y. Wang and L. You in Tsinghua University. This study is supported by NSF of China (Grants No. 12088101 and No. 11905007), and NSAF (Grants No. U1930403 and No. U1930402).

APPENDIX A: THE LOW ENERGY EFFECTIVE HAMILTONIAN OF NANOWIRE

Here we derive the effective Hamiltonian of the nanowire by using the Fröhlich-Nakajima transformation. For the hybrid semiconductor-superconductor nanowire system, the total Hamiltonian has three basic terms: $\hat{\mathcal{H}} = \hat{H}_w + \hat{H}_{sc} + \hat{H}_{w-sc}$. The nanowire Hamiltonian (1) in the continuous limit is [3]

$$\hat{H}_w = \int dx \hat{\psi}^\dagger(x) \left[-\frac{\partial_x^2}{2m_w} - \mu - i\alpha\sigma^y\partial_x + B\sigma^z \right] \hat{\psi}(x), \quad (\text{A1})$$

where $\hat{\psi}(x) = [\hat{\psi}_\uparrow(x), \hat{\psi}_\downarrow(x)]^T$, and $\sigma^{y,z}$ are the Pauli matrices. Here \uparrow, \downarrow indicate the electron spins, α is the spin-orbit coupling strength, m_w is the effective mass, μ is the chemical potential of the nanowire, and B is the Zeeman splitting from the external magnetic field, respectively. The s -wave superconductor (SC) providing the SC proximity effect for the nanowire, which is described by the BCS Hamiltonian

$$\hat{H}_{sc} = \int \frac{d^3k}{(2\pi)^3} \epsilon_{\mathbf{k}}^{\text{sc}} [\hat{c}_\uparrow^\dagger(\mathbf{k})\hat{c}_\uparrow(\mathbf{k}) - \hat{c}_\downarrow(-\mathbf{k})\hat{c}_\downarrow^\dagger(-\mathbf{k})] + \Delta_s [\hat{c}_\uparrow^\dagger(\mathbf{k})\hat{c}_\downarrow^\dagger(-\mathbf{k}) + \text{H.c.}], \quad (\text{A2})$$

with the kinetic energy $\epsilon_{\mathbf{k}}^{\text{sc}}$ and real pairing potential Δ_s of SC. The fermion operator $\hat{c}_{\uparrow,\downarrow}(\mathbf{k})$ follows the anticommutation relation $\{\hat{c}_s(\mathbf{k}), \hat{c}_{s'}^\dagger(\mathbf{k}')\}_+ = (2\pi)^3 \delta_{ss'} \delta(\mathbf{k} - \mathbf{k}')$. The tunneling interaction between the nanowire and s -wave superconductor is

$$\hat{H}_{w-sc} = -J_s \sum_s \int dx [\hat{\psi}_s^\dagger(x)\hat{c}_s(x, 0, 0) + \hat{c}_s^\dagger(x, 0, 0)\hat{\psi}_s(x)]. \quad (\text{A3})$$

Here J_s describes the tunneling strength between the nanowire and the s -wave SC, and $\hat{c}_s(\mathbf{x})$ is Fourier image of $\hat{c}_s(\mathbf{k})$:

$$\hat{c}_s(\mathbf{x}) = \frac{1}{(2\pi)^3} \int \hat{c}_s(\mathbf{k}) e^{i\mathbf{k}\cdot\mathbf{x}} d^3k. \quad (\text{A4})$$

Similarly, the above nanowire Hamiltonian (A1) and tunneling Hamiltonian (A3) in Fourier space become

$$\hat{H}_w = \int \frac{dk_x}{2\pi} \hat{\phi}^\dagger(k_x) [\epsilon_{k_x} + \alpha k_x \sigma^y + B \sigma^z] \hat{\phi}(k_x), \quad \hat{H}_{w\text{-sc}} = -J_s \sum_s \int \frac{d^3k}{(2\pi)^3} [\varphi_s^\dagger(k_x) \hat{c}_s(\mathbf{k}) + \hat{c}_s^\dagger(\mathbf{k}) \varphi_s(k_x)]. \quad (\text{A5})$$

Here $\hat{\phi}(k_x) = [\hat{\phi}_\uparrow(k_x), \hat{\phi}_\downarrow(k_x)]^T$ is obtained by Fourier transform of two-component operator $\hat{\psi}(x)$ in real space, $\epsilon_{k_x} \equiv \frac{k_x^2}{2m_w} - \mu$ is the electron kinetic energy of the nanowire, and k_x is the x component of \mathbf{k} .

By the following Bogoliubov transformation:

$$\hat{\eta}_\uparrow(\mathbf{k}) := \cos \theta_{\mathbf{k}} \hat{c}_\uparrow(\mathbf{k}) + \sin \theta_{\mathbf{k}} \hat{c}_\downarrow^\dagger(-\mathbf{k}), \quad \hat{\eta}_\downarrow^\dagger(-\mathbf{k}) := -\sin \theta_{\mathbf{k}} \hat{c}_\uparrow(\mathbf{k}) + \cos \theta_{\mathbf{k}} \hat{c}_\downarrow^\dagger(-\mathbf{k}), \quad (\text{A6})$$

with $\tan 2\theta_{\mathbf{k}} = \Delta_s / \epsilon_{\mathbf{k}}^{\text{sc}}$, the Hamiltonian of the s -wave SC can be diagonally reduced to

$$\hat{H}_{\text{sc}} = \int \frac{d^3k}{(2\pi)^3} E_{\mathbf{k}}^{\text{sc}} [\hat{\eta}_\uparrow^\dagger(\mathbf{k}) \hat{\eta}_\uparrow(\mathbf{k}) + \hat{\eta}_\downarrow^\dagger(-\mathbf{k}) \hat{\eta}_\downarrow(-\mathbf{k})], \quad (\text{A7})$$

with the excitation spectrum of the SC $E_{\mathbf{k}}^{\text{sc}} = \sqrt{[\epsilon_{\mathbf{k}}^{\text{sc}}]^2 + \Delta_s^2}$. Then the tunneling Hamiltonian $\hat{H}_{w\text{-sc}}$ [Eq. (A3)] is rewritten by the quasiparticle operators $\hat{\eta}_s(\mathbf{k})$ as

$$\begin{aligned} \hat{H}_{w\text{-sc}} = & -J_s \int \frac{d^3k}{(2\pi)^3} \{ \hat{\eta}_\uparrow(\mathbf{k}) [-\cos \theta_{\mathbf{k}} \hat{\phi}_\uparrow^\dagger(k_x) + \sin \theta_{\mathbf{k}} \hat{\phi}_\downarrow(-k_x)] + \hat{\eta}_\uparrow^\dagger(\mathbf{k}) [\cos \theta_{\mathbf{k}} \hat{\phi}_\uparrow(k_x) - \sin \theta_{\mathbf{k}} \hat{\phi}_\downarrow^\dagger(-k_x)] \\ & + \hat{\eta}_\downarrow(\mathbf{k}) [-\cos \theta_{\mathbf{k}} \hat{\phi}_\downarrow^\dagger(k_x) - \sin \theta_{\mathbf{k}} \hat{\phi}_\uparrow(-k_x)] + \hat{\eta}_\downarrow^\dagger(\mathbf{k}) [\cos \theta_{\mathbf{k}} \hat{\phi}_\downarrow(k_x) + \sin \theta_{\mathbf{k}} \hat{\phi}_\uparrow^\dagger(-k_x)] \}. \end{aligned} \quad (\text{A8})$$

In order to obtain the effective theory for the nanowire, we utilize the Fröhlich-Nakajima transformation to eliminate the quasiparticle excitation in SC. For the total Hamiltonian $\hat{\mathcal{H}} = [\hat{H}_w + \hat{H}_{\text{sc}}] + \hat{H}_{w\text{-sc}} := \hat{H}_0 + \hat{H}_1$, we apply a unitary transformation

$$\hat{H}_S = e^{-\hat{S}} \hat{H} e^{\hat{S}} = \hat{H}_0 + (\hat{H}_1 + [\hat{H}_0, \hat{S}]) + \frac{1}{2} [\hat{H}_1, \hat{S}] + \frac{1}{2} [(\hat{H}_1 + [\hat{H}_0, \hat{S}]), \hat{S}] + \dots \quad (\text{A9})$$

The anti-Hermitian operator \hat{S} should be properly set to make sure $\hat{H}_1 + [\hat{H}_0, \hat{S}] \equiv 0$, so the effective Hamiltonian becomes $\hat{H}_{\text{eff}} = \hat{H}_0 + \frac{1}{2} [\hat{H}_1, \hat{S}]$.

Specifically, here we adopt an ansatz that \hat{S} has the following form:

$$\begin{aligned} \hat{S} = & \int \frac{d^3k}{(2\pi)^3} \{ \hat{\eta}_\uparrow(\mathbf{k}) [A_{\mathbf{k}} \hat{\phi}_\uparrow^\dagger(k_x) + B_{\mathbf{k}} \hat{\phi}_\downarrow(-k_x) + E_{\mathbf{k}} \hat{\phi}_\downarrow^\dagger(k_x) + F_{\mathbf{k}} \hat{\phi}_\uparrow(-k_x)] \\ & + \hat{\eta}_\uparrow^\dagger(\mathbf{k}) [A'_{\mathbf{k}} \hat{\phi}_\uparrow(k_x) + B'_{\mathbf{k}} \hat{\phi}_\downarrow^\dagger(-k_x) + E'_{\mathbf{k}} \hat{\phi}_\downarrow(k_x) + F'_{\mathbf{k}} \hat{\phi}_\uparrow^\dagger(-k_x)] + \hat{\eta}_\downarrow(\mathbf{k}) [C_{\mathbf{k}} \hat{\phi}_\downarrow^\dagger(k_x) + D_{\mathbf{k}} \hat{\phi}_\uparrow(-k_x) + H_{\mathbf{k}} \hat{\phi}_\uparrow^\dagger(k_x) + L_{\mathbf{k}} \hat{\phi}_\downarrow(-k_x)] \\ & + \hat{\eta}_\downarrow^\dagger(\mathbf{k}) [C'_{\mathbf{k}} \hat{\phi}_\downarrow(k_x) + D'_{\mathbf{k}} \hat{\phi}_\uparrow^\dagger(-k_x) + H'_{\mathbf{k}} \hat{\phi}_\uparrow(k_x) + L'_{\mathbf{k}} \hat{\phi}_\downarrow^\dagger(-k_x)] \}. \end{aligned} \quad (\text{A10})$$

Then, by using the above Eqs. (A5), (A7), (A8), and (A10), the condition $\hat{H}_1 + [\hat{H}_0, \hat{S}] \equiv 0$ gives

$$\begin{aligned} & \int \frac{d^3k}{(2\pi)^3} \{ [(-E_{\mathbf{k}}^{\text{sc}} + \epsilon_{k_x, \downarrow}) E_{\mathbf{k}} + i\alpha k_x A_{\mathbf{k}}] \hat{\eta}_\uparrow(\mathbf{k}) \hat{\phi}_\downarrow^\dagger(k_x) - [(E_{\mathbf{k}}^{\text{sc}} - \epsilon_{k_x, \uparrow}) A_{\mathbf{k}} + i\alpha k_x E_{\mathbf{k}} - J_s \cos \theta_{\mathbf{k}}] \hat{\eta}_\uparrow(\mathbf{k}) \hat{\phi}_\uparrow^\dagger(k_x) \\ & + [(E_{\mathbf{k}}^{\text{sc}} - \epsilon_{k_x, \uparrow}) A'_{\mathbf{k}} - i\alpha k_x E'_{\mathbf{k}} - J_s \cos \theta_{\mathbf{k}}] \hat{\eta}_\uparrow^\dagger(\mathbf{k}) \hat{\phi}_\uparrow(k_x) + [(E_{\mathbf{k}}^{\text{sc}} - \epsilon_{k_x, \downarrow}) E'_{\mathbf{k}} + i\alpha k_x A'_{\mathbf{k}}] \hat{\eta}_\uparrow^\dagger(\mathbf{k}) \hat{\phi}_\downarrow(k_x) \\ & - [(E_{\mathbf{k}}^{\text{sc}} + \epsilon_{k_x, \downarrow}) B_{\mathbf{k}} + i\alpha k_x F_{\mathbf{k}} + J_s \sin \theta_{\mathbf{k}}] \hat{\eta}_\uparrow(\mathbf{k}) \hat{\phi}_\downarrow(-k_x) + [- (E_{\mathbf{k}}^{\text{sc}} + \epsilon_{k_x, \uparrow}) F_{\mathbf{k}} + i\alpha k_x B_{\mathbf{k}}] \hat{\eta}_\uparrow(\mathbf{k}) \hat{\phi}_\uparrow(-k_x) \\ & + [(E_{\mathbf{k}}^{\text{sc}} + \epsilon_{k_x, \downarrow}) B'_{\mathbf{k}} - i\alpha k_x F'_{\mathbf{k}} + J_s \sin \theta_{\mathbf{k}}] \hat{\eta}_\uparrow^\dagger(\mathbf{k}) \hat{\phi}_\downarrow^\dagger(-k_x) + [(E_{\mathbf{k}}^{\text{sc}} + \epsilon_{k_x, \uparrow}) F'_{\mathbf{k}} + i\alpha k_x B'_{\mathbf{k}}] \hat{\eta}_\uparrow^\dagger(\mathbf{k}) \hat{\phi}_\uparrow(k_x) \\ & - [(E_{\mathbf{k}}^{\text{sc}} - \epsilon_{k_x, \downarrow}) C_{\mathbf{k}} - i\alpha k_x H_{\mathbf{k}} - J_s \cos \theta_{\mathbf{k}}] \hat{\eta}_\downarrow(\mathbf{k}) \hat{\phi}_\downarrow^\dagger(k_x) + [- (E_{\mathbf{k}}^{\text{sc}} - \epsilon_{k_x, \uparrow}) H_{\mathbf{k}} - i\alpha k_x C_{\mathbf{k}}] \hat{\eta}_\downarrow(\mathbf{k}) \hat{\phi}_\uparrow^\dagger(k_x) \\ & + [(E_{\mathbf{k}}^{\text{sc}} - \epsilon_{k_x, \downarrow}) C'_{\mathbf{k}} + i\alpha k_x H'_{\mathbf{k}} - J_s \sin \theta_{\mathbf{k}}] \hat{\eta}_\downarrow^\dagger(\mathbf{k}) \hat{\phi}_\downarrow^\dagger(k_x) + [(E_{\mathbf{k}}^{\text{sc}} - \epsilon_{k_x, \uparrow}) H'_{\mathbf{k}} - i\alpha k_x C'_{\mathbf{k}}] \hat{\eta}_\downarrow^\dagger(\mathbf{k}) \hat{\phi}_\uparrow(k_x) \\ & - [(E_{\mathbf{k}}^{\text{sc}} + \epsilon_{k_x, \uparrow}) D_{\mathbf{k}} - i\alpha k_x L_{\mathbf{k}} - J_s \sin \theta_{\mathbf{k}}] \hat{\eta}_\downarrow(\mathbf{k}) \hat{\phi}_\uparrow(-k_x) + [- (E_{\mathbf{k}}^{\text{sc}} + \epsilon_{k_x, \downarrow}) L_{\mathbf{k}} - i\alpha k_x D_{\mathbf{k}}] \hat{\eta}_\downarrow(\mathbf{k}) \hat{\phi}_\downarrow(k_x) \\ & + [(E_{\mathbf{k}}^{\text{sc}} + \epsilon_{k_x, \uparrow}) D'_{\mathbf{k}} + i\alpha k_x L'_{\mathbf{k}} - J_s \sin \theta_{\mathbf{k}}] \hat{\eta}_\downarrow^\dagger(\mathbf{k}) \hat{\phi}_\uparrow^\dagger(-k_x) + [(E_{\mathbf{k}}^{\text{sc}} + \epsilon_{k_x, \downarrow}) L'_{\mathbf{k}} - i\alpha k_x D'_{\mathbf{k}}] \hat{\eta}_\downarrow^\dagger(\mathbf{k}) \hat{\phi}_\downarrow^\dagger(-k_x) \} \equiv 0, \end{aligned} \quad (\text{A11})$$

with $\epsilon_{k_x, \uparrow(\downarrow)} \equiv \epsilon_{k_x} \pm B$. The coefficients of each term in the above integral should be zero, and then the undetermined coefficients in S are solved as

$$\begin{aligned} A_{\mathbf{k}} = A'_{\mathbf{k}} &= \frac{J_s \cos \theta_{\mathbf{k}} [E_{\mathbf{k}}^{\text{sc}} - \epsilon_{k_x, \downarrow}]}{\Pi_{-}(\mathbf{k})}, & B_{\mathbf{k}} = B'_{\mathbf{k}} &= -\frac{J_s \sin \theta_{\mathbf{k}} [E_{\mathbf{k}}^{\text{sc}} + \epsilon_{k_x, \uparrow}]}{\Pi_{+}(\mathbf{k})}, & C_{\mathbf{k}} = C'_{\mathbf{k}} &= \frac{J_s \cos \theta_{\mathbf{k}} [E_{\mathbf{k}}^{\text{sc}} - \epsilon_{k_x, \uparrow}]}{\Pi_{-}(\mathbf{k})}, \\ D_{\mathbf{k}} = D'_{\mathbf{k}} &= \frac{J_s \sin \theta_{\mathbf{k}} [E_{\mathbf{k}}^{\text{sc}} + \epsilon_{k_x, \downarrow}]}{\Pi_{+}(\mathbf{k})}, & E_{\mathbf{k}} = -E'_{\mathbf{k}} = -H_{\mathbf{k}} = H'_{\mathbf{k}} &= \frac{i\alpha k_x J_s \cos \theta_{\mathbf{k}}}{\Pi_{-}(\mathbf{k})}, & F_{\mathbf{k}} = -F'_{\mathbf{k}} = L_{\mathbf{k}} = -L'_{\mathbf{k}} &= -\frac{i\alpha k_x J_s \sin \theta_{\mathbf{k}}}{\Pi_{+}(\mathbf{k})}, \end{aligned} \quad (\text{A12})$$

with $\Pi_{\pm}(\mathbf{k}) = (E_{\mathbf{k}}^{\text{sc}} \pm \epsilon_{k_x})^2 - (B^2 + \alpha^2 k_x^2)$.

When the magnetic field is not too strong and the electron tunneling strength between the nanowire and SC is weak, i.e., $|\Pi_{\pm}(\mathbf{k})| \gg (J_s k_F^s)^2$ (k_F^s is Fermi momentum of the SC), the effective Hamiltonian of the nanowire is further obtained as $\hat{H}_{\text{eff}} = \hat{H}_0 + \frac{1}{2}[\hat{H}_1, \hat{S}]$, which is calculated as follows [by using $\{\hat{\eta}_s(\mathbf{k}), \hat{\eta}_{s'}^{\dagger}(\mathbf{k}')\}_+ = (2\pi)^3 \delta_{ss'} \delta(\mathbf{k} - \mathbf{k}')$]:

$$\begin{aligned} \frac{1}{2}[\hat{H}_1, \hat{S}] &= \frac{J_s}{2} \int \frac{d^3 k}{(2\pi)^3} \{ [-\cos \theta_{\mathbf{k}} \hat{\phi}_{\uparrow}^{\dagger}(k_x) + \sin \theta_{\mathbf{k}} \hat{\phi}_{\downarrow}^{\dagger}(-k_x)] [A'_{\mathbf{k}} \hat{\phi}_{\uparrow}(k_x) + B'_{\mathbf{k}} \hat{\phi}_{\downarrow}^{\dagger}(-k_x) + E'_{\mathbf{k}} \hat{\phi}_{\downarrow}(k_x) + F'_{\mathbf{k}} \hat{\phi}_{\uparrow}^{\dagger}(-k_x)] \\ &\quad + [\cos \theta_{\mathbf{k}} \hat{\phi}_{\uparrow}(k_x) - \sin \theta_{\mathbf{k}} \hat{\phi}_{\downarrow}^{\dagger}(-k_x)] [A_{\mathbf{k}} \hat{\phi}_{\uparrow}^{\dagger}(k_x) + B_{\mathbf{k}} \hat{\phi}_{\downarrow}(-k_x) + E_{\mathbf{k}} \hat{\phi}_{\downarrow}^{\dagger}(k_x) + F_{\mathbf{k}} \hat{\phi}_{\uparrow}(-k_x)] \\ &\quad + [-\cos \theta_{\mathbf{k}} \hat{\phi}_{\downarrow}^{\dagger}(k_x) - \sin \theta_{\mathbf{k}} \hat{\phi}_{\uparrow}^{\dagger}(-k_x)] [C'_{\mathbf{k}} \hat{\phi}_{\downarrow}(k_x) + D'_{\mathbf{k}} \hat{\phi}_{\uparrow}^{\dagger}(-k_x) + H'_{\mathbf{k}} \hat{\phi}_{\uparrow}(k_x) + L'_{\mathbf{k}} \hat{\phi}_{\downarrow}^{\dagger}(-k_x)] \\ &\quad + [\cos \theta_{\mathbf{k}} \hat{\phi}_{\downarrow}(k_x) + \sin \theta_{\mathbf{k}} \hat{\phi}_{\uparrow}^{\dagger}(-k_x)] [C_{\mathbf{k}} \hat{\phi}_{\downarrow}^{\dagger}(k_x) + D_{\mathbf{k}} \hat{\phi}_{\uparrow}(-k_x) + H_{\mathbf{k}} \hat{\phi}_{\uparrow}^{\dagger}(k_x) + L_{\mathbf{k}} \hat{\phi}_{\downarrow}(-k_x)] \} \\ &= \frac{1}{2} J_s \int \frac{d^3 k}{(2\pi)^3} \{ [-2A_{\mathbf{k}} \cos \theta_{\mathbf{k}} + 2D_{\mathbf{k}} \sin \theta_{\mathbf{k}}] \hat{\phi}_{\uparrow}^{\dagger}(k_x) \hat{\phi}_{\uparrow}(k_x) + [-2B_{\mathbf{k}} \sin \theta_{\mathbf{k}} - 2C_{\mathbf{k}} \cos \theta_{\mathbf{k}}] \hat{\phi}_{\downarrow}^{\dagger}(k_x) \hat{\phi}_{\downarrow}(k_x) + [2 \cos \theta_{\mathbf{k}} E_{\mathbf{k}} \\ &\quad - 2 \sin \theta_{\mathbf{k}} F_{\mathbf{k}}] \hat{\phi}_{\uparrow}^{\dagger}(k_x) \hat{\phi}_{\downarrow}(k_x) - \hat{\phi}_{\downarrow}^{\dagger}(k_x) \hat{\phi}_{\uparrow}(k_x) + [A_{\mathbf{k}} \sin \theta_{\mathbf{k}} - B_{\mathbf{k}} \cos \theta_{\mathbf{k}} + C_{\mathbf{k}} \sin \theta_{\mathbf{k}} + D_{\mathbf{k}} \cos \theta_{\mathbf{k}}] [\hat{\phi}_{\uparrow}^{\dagger}(k_x) \hat{\phi}_{\downarrow}^{\dagger}(-k_x) \\ &\quad + \hat{\phi}_{\downarrow}(-k_x) \hat{\phi}_{\uparrow}(k_x)] + [\sin \theta_{\mathbf{k}} E_{\mathbf{k}} + \cos \theta_{\mathbf{k}} F_{\mathbf{k}}] [\hat{\phi}_{\uparrow}^{\dagger}(k_x) \hat{\phi}_{\uparrow}^{\dagger}(-k_x) - \hat{\phi}_{\uparrow}(-k_x) \hat{\phi}_{\uparrow}(k_x) + \hat{\phi}_{\downarrow}^{\dagger}(k_x) \hat{\phi}_{\downarrow}^{\dagger}(-k_x) - \hat{\phi}_{\downarrow}(-k_x) \hat{\phi}_{\downarrow}(k_x)] \}. \end{aligned} \quad (\text{A13})$$

Finally, by substituting the coefficients obtained in Eq. (A12) here, the effective Hamiltonian is obtained:

$$\begin{aligned} \hat{H}_{\text{eff}} &= \int \frac{dk}{2\pi} \{ \tilde{\epsilon}_k [\hat{\phi}_{\uparrow}^{\dagger}(k_x) \hat{\phi}_{\uparrow}(k_x) + \hat{\phi}_{\downarrow}^{\dagger}(k_x) \hat{\phi}_{\downarrow}(k_x)] + i\tilde{\alpha}_{k_x} [\hat{\phi}_{\downarrow}^{\dagger}(k_x) \hat{\phi}_{\uparrow}(k_x) - \text{H.c.}] \\ &\quad + \tilde{B}_{k_x} [\hat{\phi}_{\uparrow}^{\dagger}(k_x) \hat{\phi}_{\uparrow}(k_x) - \hat{\phi}_{\downarrow}^{\dagger}(k_x) \hat{\phi}_{\downarrow}(k_x)] + \tilde{\Delta}_{k_x} [\hat{\phi}_{\uparrow}^{\dagger}(k_x) \hat{\phi}_{\downarrow}^{\dagger}(-k_x) + \text{H.c.}] + \tilde{\Lambda}_{k_x} [\hat{\phi}_{\downarrow}^{\dagger}(k_x) \hat{\phi}_{\downarrow}^{\dagger}(-k_x) + \hat{\phi}_{\uparrow}^{\dagger}(k_x) \hat{\phi}_{\uparrow}^{\dagger}(-k_x) - \text{H.c.}] \}. \end{aligned} \quad (\text{A14})$$

The electron tunneling between the nanowire and the s -wave SC modifies the kinetic energy $\tilde{\epsilon}_{k_x}$, Zeeman splitting \tilde{B}_{k_x} , and spin-orbit coupling $\tilde{\alpha}_{k_x}$, and these parameters are

$$\begin{aligned} \tilde{B}_{k_x} &= \left[1 - J_s^2 \int \frac{dk_y dk_z}{(2\pi)^2} \left(\frac{\cos^2 \theta_{\mathbf{k}}}{\Pi_{-}(\mathbf{k})} + \frac{\sin^2 \theta_{\mathbf{k}}}{\Pi_{+}(\mathbf{k})} \right) \right] B, & \tilde{\alpha}_{k_x} &= \left[1 - J_s^2 \int \frac{dk_y dk_z}{(2\pi)^2} \left(\frac{\cos^2 \theta_{\mathbf{k}}}{\Pi_{-}(\mathbf{k})} + \frac{\sin^2 \theta_{\mathbf{k}}}{\Pi_{+}(\mathbf{k})} \right) \right] \alpha, \\ \tilde{\epsilon}_{k_x} &= \epsilon_{k_x} - J_s^2 \int \frac{dk_y dk_z}{(2\pi)^2} \left[\frac{\cos^2 \theta_{\mathbf{k}} E_{-}^s(\mathbf{k})}{\Pi_{-}(\mathbf{k})} - \frac{\sin^2 \theta_{\mathbf{k}} E_{+}^s(\mathbf{k})}{\Pi_{+}(\mathbf{k})} \right], & \tilde{\Delta}_{k_x} &= J_s^2 \int \frac{dk_y dk_z}{(2\pi)^2} \frac{\sin 2\theta_{\mathbf{k}}}{2} \left[\frac{E_{-}^s(\mathbf{k})}{\Pi_{-}(\mathbf{k})} + \frac{E_{+}^s(\mathbf{k})}{\Pi_{+}(\mathbf{k})} \right], \\ \tilde{\Lambda}_{k_x} &= J_s^2 \int \frac{dk_y dk_z}{(2\pi)^2} \frac{i\alpha k_x \sin 2\theta_{\mathbf{k}}}{4} \left(\frac{1}{\Pi_{-}(\mathbf{k})} - \frac{1}{\Pi_{+}(\mathbf{k})} \right), \end{aligned} \quad (\text{A15})$$

where $E_{\pm}^s(\mathbf{k}) \equiv E_{\mathbf{k}}^{\text{sc}} \pm \epsilon_{k_x}$, and $\Pi_{\pm}(\mathbf{k})$, $\sin \theta_{\mathbf{k}}$, $\cos \theta_{\mathbf{k}}$ have been given in Eqs. (A6) and (A12), respectively.

To further calculate the integrals in the above result, we consider that the Zeeman splitting B and spin-orbital coupling α of the nanowire are much smaller than the s -wave SC gap, thus $|E_{\mathbf{k}}^{\text{sc}} - \sqrt{B^2 + \alpha^2 k_x^2}| \gg |\epsilon_{k_x}|$. Then in the above integrals we omit the second and higher-order terms of $|\alpha k_x|/|E_{\mathbf{k}}^{\text{sc}} + \sqrt{B^2 + \alpha^2 k_x^2}|$ and $|\epsilon_{k_x}|/|E_{\mathbf{k}}^{\text{sc}} - \sqrt{B^2 + \alpha^2 k_x^2}|$, and the above parameters in Eq. (A15) are simplified as

$$\tilde{\Delta}_{k_x} = \Upsilon_s \left(1 - \frac{\alpha^2 k_x^2 + B^2}{\Delta_s^2} \right)^{-\frac{1}{2}}, \quad \tilde{\Lambda}_{k_x} = 0, \quad \frac{\tilde{B}_{k_x}}{B} = \frac{\tilde{\alpha}_{k_x}}{\alpha} = \frac{\tilde{\epsilon}_{k_x}}{\epsilon_{k_x}} = \frac{\tilde{\mu}_{k_x}}{\mu} = 1 - \frac{\tilde{\Delta}_{k_x}}{\Delta_s}. \quad (\text{A16})$$

Here $\Upsilon_s = J_s^2 \rho_s$ describes the coupling strength between the s -wave SC and the nanowire, where ρ_s is the two-dimensional superconducting density of states. Now we have obtained the effective Hamiltonian of the nanowire in the main text, i.e.,

$$\begin{aligned} \hat{H}_{\text{eff}} = & \int \frac{dk_x}{2\pi} \{ \tilde{\epsilon}_{k_x} [\hat{\phi}_\uparrow^\dagger(k_x) \hat{\phi}_\uparrow(k_x) + \hat{\phi}_\downarrow^\dagger(k_x) \hat{\phi}_\downarrow(k_x)] + i\tilde{\alpha}_{k_x} k_x [\hat{\phi}_\downarrow^\dagger(k_x) \hat{\phi}_\uparrow(k_x) - \text{H.c.}] \\ & + \tilde{B}_{k_x} [\hat{\phi}_\uparrow^\dagger(k_x) \hat{\phi}_\uparrow(k_x) - \hat{\phi}_\downarrow^\dagger(k_x) \hat{\phi}_\downarrow(k_x)] + \tilde{\Delta}_{k_x} [\hat{\phi}_\uparrow^\dagger(k_x) \hat{\phi}_\downarrow^\dagger(-k_x) + \text{H.c.}] \}. \end{aligned} \quad (\text{A17})$$

Clearly, $\tilde{\Delta}_{k_x}$ is the pairing potential induced by the SC proximity effect, and all these parameters $\tilde{\epsilon}_{k_x}$, $\tilde{\alpha}_{k_x}$, \tilde{B}_{k_x} , $\tilde{\Delta}_{k_x}$ exhibit significant dependence on the magnetic field. In addition, when the SC gap is so large that $|E_{\mathbf{k}}^{\text{sc}}| \gg B$, Υ_s , in the low energy regime ($k \simeq 0$), the induced pairing strength can be approximated as a constant $\tilde{\Delta} \simeq \Upsilon_s$, and the kinetic energy, spin-orbital coupling and Zeeman splitting of the nanowire are corrected by the constant factor $1 - \Upsilon_s/\Delta_s$ according to (A16).

Then the quasiparticle energy spectrum determined by the effective Hamiltonian in Eq. (A17) is

$$E_{\pm}(k_x) = \sqrt{\tilde{\Delta}_{k_x}^2 + \frac{\tilde{\epsilon}_{k_x,+}^2 + \tilde{\epsilon}_{k_x,-}^2}{2} \pm (\tilde{\epsilon}_{k_x,+} - \tilde{\epsilon}_{k_x,-}) \sqrt{[\tilde{\Delta}_{k_x}^{(s)}]^2 + \tilde{\epsilon}_{k_x}^2}}, \quad (\text{A18})$$

with $\tilde{\epsilon}_{k_x,\pm} = \tilde{\epsilon}_{k_x} \pm \sqrt{\tilde{B}_{k_x}^2 + \tilde{\alpha}_{k_x}^2 k_x^2}$ and $\tilde{\Delta}_{k_x}^{(s)} = B \tilde{\Delta}_{k_x} / \sqrt{B^2 + \alpha^2 k_x^2}$. The energy level crossing point of the quasiparticle energy spectrum is $E_-(k_x = 0) = 0$, which gives the critical condition of topological phase: $\tilde{B}_{k_x=0} = \sqrt{\tilde{\mu}_{k_x=0}^2 + \tilde{\Delta}_{k_x=0}^2}$. When the corrected magnetic field satisfies

$$\tilde{B}_{k_x=0}(B, \Upsilon_s) > \sqrt{\tilde{\mu}_{k_x=0}^2(B, \Upsilon_s) + \tilde{\Delta}_{k_x=0}^2(B, \Upsilon_s)}, \quad (\text{A19})$$

the energy gap reopens, and the topological phase with Majorana zero modes emerges in the region [3,41]. However, when the magnetic field gets stronger, the corrected magnetic field decreases significantly according to Eq. (A16), which makes the corrected magnetic field become $\tilde{B}_{k_x=0} < \sqrt{\tilde{\mu}_{k_x=0}^2 + \tilde{\Delta}_{k_x=0}^2}$. Then the topological phase disappear. Therefore, the topological phase only emerges at proper magnetic field strength.

APPENDIX B: MAJORANA ZERO MODES DETERMINED BY THE EFFECTIVE HAMILTONIAN OF THE NANOWIRE

Here, based on the effective Hamiltonian of the nanowire, we give the region of the existence of Majorana zero modes in the μ - B diagram, which is consistent with the topological phase region given by Eq. (A19). In the continuous limit, the effective Hamiltonian (A17) of the nanowire in the low energy regime ($k_x \simeq 0$) becomes

$$\hat{H}_{\text{eff}} = \int dx \hat{\Psi}^\dagger(x) [1 - Z(B)] \left[-\frac{\partial_x^2}{2m_w} - \mu - i\alpha\sigma^y \partial_x + B\sigma^z \right] \hat{\Psi}(x) + Z(B) \Delta_s [\hat{\psi}_\uparrow^\dagger(x) \hat{\psi}_\downarrow^\dagger(x) + \hat{\psi}_\downarrow(x) \hat{\psi}_\uparrow(x)], \quad (\text{B1})$$

where the corrected factor is defined as $Z(B) \equiv \frac{\Upsilon_s}{\Delta_s} (1 - \frac{B^2}{\Delta_s^2})^{-\frac{1}{2}}$. In the Nambu representation, the above Hamiltonian becomes

$$\hat{H}_{\text{eff}} = \frac{1}{2} \int dx \hat{\Phi}^\dagger(x) \cdot \mathbf{H}_x \cdot \hat{\Phi}(x), \quad (\text{B2})$$

with $\hat{\Phi}(x) = [\hat{\psi}(x), \hat{\psi}^\dagger(x)]^T$ as the four-component operator and

$$\mathbf{H}_x = \begin{bmatrix} [1 - Z(B)] \left(-\frac{\partial_x^2}{2m_w} - \mu - i\alpha\sigma^y \partial_x + B\sigma^z \right) & i\sigma^y Z(B) \Delta_s \\ -i\sigma^y Z(B) \Delta_s & [1 - Z(B)] \left(\frac{\partial_x^2}{2m_w} + \mu + i\alpha\sigma^y \partial_x - B\sigma^z \right) \end{bmatrix}. \quad (\text{B3})$$

Considering the Bogoliubov–de Gennes (BdG) equation

$$\mathbf{H}_x \Psi_E(x) = E \Psi_E(x), \quad (\text{B4})$$

the corresponding wave function is $\Psi_E(x) = [u_{\uparrow,E}(x), u_{\downarrow,E}(x), v_{\uparrow,E}(x), v_{\downarrow,E}(x)]^T$. Then the effective Hamiltonian (B1) is diagonalized as $H_{\text{eff}} = \frac{1}{2} \sum_E E \hat{\gamma}_E^\dagger \hat{\gamma}_E$, where

$$\hat{\gamma}_E = \int dx \sum_s [u_{s,E}^*(x) \hat{\psi}_s(x) + v_{s,E}^*(x) \hat{\psi}_s^\dagger(x)]. \quad (\text{B5})$$

For the Majorana fermion, the antiparticle is itself, which means the quasiparticle operator is self-Hermitian $\hat{\gamma}_E = \hat{\gamma}_E^\dagger$, that is,

$$u_{s,E}(x) = v_{s,E}^*(x). \quad (\text{B6})$$

And due to the particle-hole symmetry of the system, the single-particle Hamiltonian satisfies $\sigma^x \mathbf{H}_x^T \sigma^x = -\mathbf{H}_x$. So $\sigma^x \Psi_E^*(x)$ is the eigenstate of the single-particle Hamiltonian for the energy $-E$:

$$\mathbf{H}_x[\sigma^x \Psi_E^*(x)] = -E[\sigma^x \Psi_E^*(x)]. \quad (\text{B7})$$

Correspondingly, the quasiparticle operator is

$$\hat{\gamma}_{-E} = \int dx \sum_s [v_{s,E} \hat{\psi}_s(x) + u_{s,E}(x) \hat{\psi}_s^\dagger(x)]. \quad (\text{B8})$$

If the wave function $\Psi_E(x)$ is nondegenerate, we obtain relation of $u_{s,E}(x)$ and $v_{s,E}(x)$ by Eqs. (B5) and (B8) again, i.e.,

$$u_{s,E}(x) = v_{s,-E}^*(x). \quad (\text{B9})$$

Due to the self-Hermitian relation of the Majorana fermion (B6) and the particle-hole symmetry of the system (B9), the components of the wave function $u_{s,E}(x)$ and $v_{s,E}(x)$ satisfy

$$u_{s,E}(x) = u_{s,-E}(x). \quad (\text{B10})$$

Thus, only the zero mode quasiparticle could be self-Hermitian, i.e., the Majorana zero mode.

For $E = 0$, considering that the Majorana fermion requires $u_{s,E}(x) = v_{s,E}^*(x)$, the BdG equation (B4) is reduced to

$$[1 - Z(B)] \left(-\frac{\partial_x^2}{2m_w} - \mu - i\alpha\sigma^y \partial_x + B\sigma^z \right) \mathbf{u}(x) + i\sigma^y Z(B) \Delta_s \mathbf{u}^*(x) = 0, \quad (\text{B11})$$

with the two-component wave function $\mathbf{u}(x) \equiv [u_\uparrow(x), u_\downarrow(x)]^T$. Here we consider the length of the nanowire is L , and $x \in [0, L]$. Then $\mathbf{u}(x)$ can be decomposed into the real and imaginary parts $\mathbf{u}(x) = \mathbf{u}^{(r)}(x) + i\mathbf{u}^{(i)}(x)$, and we assume they have the following forms:

$$\mathbf{u}^{(r)}(x) = e^{-\xi_r x} [u_\uparrow^{(r)}, u_\downarrow^{(r)}]^T, \quad \mathbf{u}^{(i)}(x) = e^{-\xi_i x} [u_\uparrow^{(i)}, u_\downarrow^{(i)}]^T, \quad (\text{B12})$$

where ξ_r and ξ_i are real numbers. Taking the ansatz (B12) into the reduced BdG equation (B11), we get the equations of the real and imaginary parts respectively,

$$\begin{bmatrix} -\frac{\xi_r^2}{2m_w} - \mu + B & (-\alpha\xi_r + \frac{Z(B)}{1-Z(B)}\Delta_s) \\ (\alpha\xi_r - \frac{Z(B)}{1-Z(B)}\Delta_s) & -\frac{\xi_r^2}{2m_w} - \mu - B \end{bmatrix} \mathbf{u}^{(r)}(x) = 0, \quad \begin{bmatrix} -\frac{\xi_i^2}{2m_w} - \mu + B & (-\alpha\xi_i - \frac{Z(B)}{1-Z(B)}\Delta_s) \\ (\alpha\xi_i + \frac{Z(B)}{1-Z(B)}\Delta_s) & -\frac{\xi_i^2}{2m_w} - \mu - B \end{bmatrix} \mathbf{u}^{(i)}(x) = 0. \quad (\text{B13})$$

If the above two equations have solutions, the determinants of the coefficient matrices in Eq. (B13) are zero:

$$0 = \left[-\frac{1}{2m_w} \xi_r^2 - \mu \right]^2 + \left(\alpha\xi_r - \frac{Z(B)}{1-Z(B)} \Delta_s \right)^2 - B^2 \equiv f(\xi_r), \quad (\text{B14})$$

$$0 = \left[-\frac{1}{2m_w} \xi_i^2 - \mu \right]^2 + \left(\alpha\xi_i + \frac{Z(B)}{1-Z(B)} \Delta_s \right)^2 - B^2 \equiv g(\xi_i). \quad (\text{B15})$$

Here the parameters μ , m_w , α , and B are all positive, and the corrected factor satisfies $0 < Z(B) < 1$, and thus $Z(B)/[1 - Z(B)] > 0$.

(a) If the equation $f(\xi) = 0$ has a positive root $\xi_r > 0$, the real part $\mathbf{u}^{(r)}(x)$ has a solution localized around the end $x = 0$. The existence condition for ξ_r can be given by examining the monotonicity $f(\xi)$. Notice that the quartic function $f(\xi)$ satisfies

$$f''(\xi) = \frac{1}{m_w} \left[\frac{3}{m_w} \xi^2 + 2\mu \right] + 2\alpha^2 > 0, \quad (\text{B16})$$

thus $f'(\xi)$ is monotonically increasing. Thus, in the interval $\xi \in [0, \infty)$, the minimum of $f'(\xi)$ appears at $\xi = 0$, which is $f'(0) = -2\alpha Z(B) \Delta_s / [1 - Z(B)] < 0$. Therefore, there must exist a certain $\xi_0 > 0$ satisfying $f'(\xi_0) = 0$, that means, when $0 \leq \xi < \xi_0$, $f(\xi)$ is monotonically decreasing, and when $\xi > \xi_0$, $f(\xi)$ is monotonically increasing. Namely, the minimum of $f(\xi)$ appears at ξ_0 . To make sure Eq. (B14) have one solution or two solutions, we must have $\min f(\xi) = f(\xi_0) < 0$.

(b) If the equation $g(\xi) = 0$ has a positive root $\xi_i > 0$, the imaginary part $\mathbf{u}^{(i)}(x)$ has a solution localized around the end $x = 0$. In the interval $\xi \in [0, \infty)$, $g'(\xi)$ is always positive, i.e.,

$$g'(\xi) = \frac{2\xi}{m_w} \left[\frac{1}{2m_w} \xi^2 + \mu \right] + 2\alpha \left(\alpha\xi + \frac{Z(B)}{1-Z(B)} \Delta_s \right) > 0, \quad (\text{B17})$$

thus $g(\xi)$ is monotonically increasing. Therefore, to make sure Eq. (B15) has a solution, we must have $\min g(\xi) = g(0) < 0$.

Now combining the two existence conditions from (a) and (b), since $\min g(\xi) = g(0) = f(0) > \min f(\xi)$, to make sure both $\mathbf{u}^{(r)}(x)$ and $\mathbf{u}^{(i)}(x)$ have solutions, we must have $\min g(\xi) = g(0) < 0$, and that gives

$$B > \sqrt{\mu^2 + \left[\frac{Z(B)}{1 - Z(B)} \Delta_s \right]^2}. \quad (\text{B18})$$

Similarly, it is also proved that there is an edge state around the other end ($x = L$) if Eq. (B18) is satisfied, which means the existence of the Majorana zero modes localized at the two ends. Notice that this condition is just the same with the topological phase criterion (A19) obtained from the crossing point of the quasiparticle energy spectrum.

APPENDIX C: HAMILTONIAN DESCRIPTION FOR THE NANOWIRE SYSTEM

Now we study the transport behavior of the nanowire system. We consider the nanowire is contacted with two electron leads at the two ends, and then derive a quantum Langevin equation to describe the dynamics of the nanowire. First, the Hamiltonian (A1) of the nanowire is discretized as N sites, that is

$$\hat{H}_w = \sum_{n,s} -\frac{J}{2} (\hat{d}_{n,s}^\dagger \hat{d}_{n+1,s} + \hat{d}_{n+1,s}^\dagger \hat{d}_{n,s}) - (\mu - J) \hat{d}_{n,s}^\dagger \hat{d}_{n,s} + \sum_n \frac{\alpha_R}{2} (\hat{d}_{n,\downarrow}^\dagger \hat{d}_{n+1,\uparrow} - \hat{d}_{n,\uparrow}^\dagger \hat{d}_{n+1,\downarrow} + \text{H.c.}) + \sum_n B (\hat{d}_{n,\uparrow}^\dagger \hat{d}_{n,\uparrow} - \hat{d}_{n,\downarrow}^\dagger \hat{d}_{n,\downarrow}). \quad (\text{C1})$$

Here $s = \uparrow, \downarrow$ indexes the electron spin, α_R indicates the spin-orbit coupling strength, J is the hopping amplitude, μ is the chemical potential of the nanowire, and B is the Zeeman splitting from the external magnetic field.

All the N sites are contacted with an s -wave SC independently, and two electron leads are contacted with site 1 and site N . The s -wave SC and the two leads are treated as the fermion baths of the nanowire, and they are described by

$$\hat{H}_{sc} = \sum_{\mathbf{k}} \epsilon_{\mathbf{k}}^{\text{sc}} (\hat{c}_{\mathbf{k}\uparrow}^\dagger \hat{c}_{\mathbf{k}\uparrow} - \hat{c}_{-\mathbf{k}\downarrow}^\dagger \hat{c}_{-\mathbf{k}\downarrow}^\dagger) + \Delta_s (\hat{c}_{\mathbf{k}\uparrow}^\dagger \hat{c}_{-\mathbf{k}\downarrow}^\dagger + \text{H.c.}), \quad \hat{H}_{e-x} = \sum_{\mathbf{k}s} \epsilon_{x,\mathbf{k}} \hat{b}_{x,\mathbf{k}s}^\dagger \hat{b}_{x,\mathbf{k}s} \quad (x = 1, N). \quad (\text{C2})$$

Both the leads and the s -wave SC are coupled with the nanowire through the tunneling interaction [see also Eq. (A3)],

$$\hat{H}_{w\text{-sc}} = - \sum_{n,\mathbf{k}s} (J_{n,\mathbf{k}} \hat{d}_{n,s}^\dagger \hat{c}_{\mathbf{k}s} + \text{H.c.}), \quad \hat{H}_{w-x} = - \sum_{\mathbf{k}s} (\mathbf{g}_{x,\mathbf{k}} \hat{d}_{x,s}^\dagger \hat{b}_{x,\mathbf{k}s} + \text{H.c.}). \quad (\text{C3})$$

Denoting $[\hat{\mathbf{d}}(t)]_{1 \times 4N} := (\hat{\mathbf{d}}_1, \dots, \hat{\mathbf{d}}_N)^T$ with blocks $[\hat{\mathbf{d}}_n]_{1 \times 4} := (\hat{d}_{n\uparrow}, \hat{d}_{n\downarrow}, \hat{d}_{n\uparrow}^\dagger, \hat{d}_{n\downarrow}^\dagger)^T$, $\hat{\mathbf{c}}_{\mathbf{k}}(t) := (\hat{c}_{\mathbf{k}\uparrow}, \hat{c}_{-\mathbf{k}\downarrow}, \hat{c}_{\mathbf{k}\uparrow}^\dagger, \hat{c}_{-\mathbf{k}\downarrow}^\dagger)^T$, and $\hat{\mathbf{b}}_{x,\mathbf{k}}(t) := (\hat{b}_{x,\mathbf{k}\uparrow}, \hat{b}_{x,\mathbf{k}\downarrow}, \hat{b}_{x,\mathbf{k}\uparrow}^\dagger, \hat{b}_{x,\mathbf{k}\downarrow}^\dagger)^T$, the above Hamiltonians (C1) and (C2) can be rewritten as

$$\hat{H}_w = \frac{1}{2} \hat{\mathbf{d}}^\dagger \cdot \mathbf{H}_w \cdot \hat{\mathbf{d}}, \quad \hat{H}_{sc} = \frac{1}{2} \sum_{\mathbf{k}} \hat{\mathbf{c}}_{\mathbf{k}}^\dagger \cdot \mathbf{H}_{\mathbf{k}}^{\text{sc}} \cdot \hat{\mathbf{c}}_{\mathbf{k}}, \quad \hat{H}_{e-x} = \frac{1}{2} \hat{\mathbf{b}}_{x,\mathbf{k}}^\dagger \cdot \mathbf{H}_{\mathbf{k}}^{e-x} \cdot \hat{\mathbf{b}}_{x,\mathbf{k}},$$

$$\mathbf{H}_{\mathbf{k}}^{\text{sc}} := \begin{bmatrix} \epsilon_{\mathbf{k}}^{\text{sc}} & & & \Delta_s \\ & \epsilon_{\mathbf{k}}^{\text{sc}} & -\Delta_s & \\ & -\Delta_s & -\epsilon_{\mathbf{k}}^{\text{sc}} & \\ \Delta_s & & & -\epsilon_{\mathbf{k}}^{\text{sc}} \end{bmatrix}, \quad \mathbf{H}_{\mathbf{k}}^{e-x} := \begin{bmatrix} \epsilon_{x,\mathbf{k}} & & & \\ & \epsilon_{x,\mathbf{k}} & & \\ & & -\epsilon_{x,\mathbf{k}} & \\ & & & -\epsilon_{x,\mathbf{k}} \end{bmatrix}. \quad (\text{C4})$$

The system dynamics can be given by the Heisenberg equation. Here we consider all the dynamical observables are corrected as $\hat{\delta}(t) = \hat{\delta}(t) \Theta(t) e^{-\epsilon t} := \hat{\delta}(t) \Theta^{(\epsilon)}(t)$ with $\epsilon \rightarrow 0$, namely, the dynamical evolution starts from $t = 0$. The infinitesimal ϵ guarantees the convergence of the evolution, and would naturally lead to the causality in the dynamical propagator. Then the equations of motions becomes $\partial_t [\hat{\delta}(t) \Theta^{(\epsilon)}(t)] = \delta(t) \hat{\delta}(0) - i \Theta^{(\epsilon)}(t) [\hat{\delta}, \hat{\mathcal{H}}]$, with $\hat{\delta}(0)$ as the initial state. Then the dynamics for the nanowire $\hat{d}_{n,s}$, s -wave SC $\hat{c}_{\mathbf{k}s}$, and electron leads $\hat{b}_{x,\mathbf{k}s}$ are given as

$$\partial_t \hat{d}_{n,s} = \delta(t) \hat{d}_{n,s}(0) - i [\hat{d}_{n,s}, \hat{H}_w] + i \sum_{\mathbf{k}} J_{n,\mathbf{k}} \hat{c}_{\mathbf{k},s} + i \sum_{x=1,N} \sum_{\mathbf{k}} \mathbf{g}_{x,\mathbf{k}} \hat{b}_{x,\mathbf{k}s}, \quad \partial_t \hat{c}_{\mathbf{k},s} = \delta(t) \hat{c}_{\mathbf{k},s}(0) - i [\hat{c}_{\mathbf{k},s}, \hat{H}_{sc}] + i \sum_n J_{n,\mathbf{k}}^* \hat{d}_{n,s},$$

$$\partial_t \hat{b}_{x,\mathbf{k}s} = \delta(t) \hat{b}_{x,\mathbf{k}s}(0) - i \epsilon_{x,\mathbf{k}} \hat{b}_{x,\mathbf{k}s} + i \mathbf{g}_{x,\mathbf{k}}^* \hat{d}_{x,s}. \quad (\text{C5})$$

These dynamical equations can be solved in the Fourier space. We adopt the following Fourier transform:

$$\hat{\delta}(t) = \int_{-\infty}^{\infty} \frac{d\omega}{2\pi} \tilde{\delta}(\omega) e^{-i\omega t}, \quad \tilde{\delta}(\omega) = \int_{-\infty}^{\infty} dt \hat{\delta}(t) e^{+i\omega t}, \quad \hat{\delta}^\dagger(t) = \int_{-\infty}^{\infty} \frac{d\omega}{2\pi} [\tilde{\delta}(\omega)]^\dagger e^{+i\omega t} = \int_{-\infty}^{\infty} \frac{d\bar{\omega}}{2\pi} \tilde{\delta}^\dagger(-\bar{\omega}) e^{-i\bar{\omega} t}. \quad (\text{C6})$$

Under this convention, the Fourier images for the vectors $\hat{\mathbf{d}}_n(t)$, $\hat{\mathbf{c}}_{\mathbf{k}}(t)$, $\hat{\mathbf{b}}_{x,\mathbf{k}}(t)$ read

$$\tilde{\mathbf{d}}_n(\omega) = (\tilde{d}_{n\uparrow}(\omega), \tilde{d}_{n\downarrow}(\omega), \tilde{d}_{n\uparrow}^\dagger(-\omega), \tilde{d}_{n\downarrow}^\dagger(-\omega))^T, \quad \tilde{\mathbf{c}}_{\mathbf{k}}(\omega) = (\tilde{c}_{\mathbf{k}\uparrow}(\omega), \tilde{c}_{-\mathbf{k}\downarrow}(\omega), \tilde{c}_{\mathbf{k}\uparrow}^\dagger(-\omega), \tilde{c}_{-\mathbf{k}\downarrow}^\dagger(-\omega))^T,$$

$$\tilde{\mathbf{b}}_{x,\mathbf{k}}(\omega) = (\tilde{b}_{x,\mathbf{k}\uparrow}(\omega), \tilde{b}_{x,\mathbf{k}\downarrow}(\omega), \tilde{b}_{x,\mathbf{k}\uparrow}^\dagger(-\omega), \tilde{b}_{x,\mathbf{k}\downarrow}^\dagger(-\omega))^T. \quad (\text{C7})$$

Then the Fourier images of the dynamical equations (C5) become ($\omega^+ := \omega + i\epsilon$)

$$\begin{aligned} -i\omega^+ \tilde{\mathbf{d}}(\omega) &= \hat{\mathbf{d}}(0) - i\mathbf{H}_w \cdot \tilde{\mathbf{d}}(\omega) + i \sum_{\mathbf{k}} [\mathbf{T}_{\mathbf{k}}]_{4N \times 4} \cdot \tilde{\mathbf{c}}_{\mathbf{k}}(\omega) + i \sum_{x=1,N} \sum_{\mathbf{k}} [\mathbf{Y}_{x,\mathbf{k}}]_{4N \times 4} \cdot \tilde{\mathbf{b}}_{x,\mathbf{k}}(\omega), \\ -i\omega^+ \tilde{\mathbf{c}}_{\mathbf{k}}(\omega) &= \hat{\mathbf{c}}_{\mathbf{k}}(0) - i\mathbf{H}_{sc}(\mathbf{k}) \cdot \tilde{\mathbf{c}}_{\mathbf{k}}(\omega) + i[\mathbf{T}_{\mathbf{k}}^\dagger]_{4 \times 4N} \cdot \tilde{\mathbf{d}}(\omega), \quad -i\omega^+ \tilde{\mathbf{b}}_{x,\mathbf{k}}(\omega) = \hat{\mathbf{b}}_{x,\mathbf{k}}(0) - i\mathbf{H}_{e-x}(\mathbf{k}) \cdot \tilde{\mathbf{b}}_{x,\mathbf{k}}(\omega) + i[\mathbf{Y}_{x,\mathbf{k}}^\dagger]_{4 \times 4N} \cdot \tilde{\mathbf{d}}(\omega). \end{aligned} \quad (\text{C8})$$

Here $\mathbf{T}_{\mathbf{k}}$ and $\mathbf{Y}_{x,\mathbf{k}}$ are the the $4N \times 4$ tunneling matrices indicating the coupling with the s -wave SC and lead- x respectively, and they are defined by

$$\mathbf{T}_{\mathbf{k}} := [\mathbf{T}_{1,\mathbf{k}}, \mathbf{T}_{2,\mathbf{k}}, \dots, \mathbf{T}_{N,\mathbf{k}}]^T, \quad \mathbf{Y}_{1,\mathbf{k}} := [\mathbf{Y}_{1,\mathbf{k}}, \mathbf{0}, \dots, \mathbf{0}]^T, \quad \mathbf{Y}_{N,\mathbf{k}} := [\mathbf{0}, \dots, \mathbf{0}, \mathbf{Y}_{N,\mathbf{k}}]^T, \quad (\text{C9})$$

with 4×4 blocks $\mathbf{T}_{n,\mathbf{k}} := \text{diag}\{J_{n,\mathbf{k}}, J_{n,\mathbf{k}}, -J_{n,-\mathbf{k}}^*, -J_{n,-\mathbf{k}}^*\}$ and $\mathbf{Y}_{x,\mathbf{k}} := \text{diag}\{g_{x,\mathbf{k}}, g_{x,\mathbf{k}}, -g_{x,\mathbf{k}}^*, -g_{x,\mathbf{k}}^*\}$.

The dynamics for the s -wave SC and the two electron leads can be formally obtained with the help of Green functions

$$\begin{aligned} \tilde{\mathbf{c}}_{\mathbf{k}}(\omega) &= \mathbf{G}_{sc}(\omega, \mathbf{k}) \cdot [\hat{\mathbf{c}}_{\mathbf{k}}(0) + i\mathbf{T}_{\mathbf{k}}^\dagger \cdot \tilde{\mathbf{d}}(\omega)], \quad \mathbf{G}_{sc}(\omega, \mathbf{k}) := i[\omega^+ - \mathbf{H}_{\mathbf{k}}^{sc}]_{4 \times 4}^{-1}, \\ \tilde{\mathbf{b}}_{x,\mathbf{k}}(\omega) &= \mathbf{G}_{e-x}(\omega, \mathbf{k}) \cdot [\hat{\mathbf{b}}_{x,\mathbf{k}}(0) + i\mathbf{Y}_{x,\mathbf{k}}^\dagger \cdot \tilde{\mathbf{d}}(\omega)], \quad \mathbf{G}_{e-x}(\omega, \mathbf{k}) := i[\omega^+ - \mathbf{H}_{\mathbf{k}}^{e-x}]_{4 \times 4}^{-1}. \end{aligned} \quad (\text{C10})$$

The Green function of lead x is $\mathbf{G}_{e-x}(\omega) = i \text{diag}\{(\omega^+ - \varepsilon_{x,\mathbf{k}})^{-1}, (\omega^+ - \varepsilon_{x,\mathbf{k}})^{-1}, (\omega^+ + \varepsilon_{x,\mathbf{k}})^{-1}, (\omega^+ + \varepsilon_{x,\mathbf{k}})^{-1}\}$, while $\mathbf{G}_{sc}(\omega)$ for the s -wave SC requires calculating the inverse of the Hamiltonian matrix $\mathbf{H}_{\mathbf{k}}^{sc}$. Taking $\tilde{\mathbf{c}}_{\mathbf{k}}(\omega)$, $\tilde{\mathbf{b}}_{x,\mathbf{k}}(\omega)$ back into the equation of $\tilde{\mathbf{d}}(\omega)$, the dynamics of the nanowire becomes

$$-i\omega^+ \tilde{\mathbf{d}}(\omega) = \hat{\mathbf{d}}(0) - i\mathbf{H}_w \cdot \tilde{\mathbf{d}}(\omega) - [\tilde{\mathbf{D}}_{sc}(\omega) + \tilde{\mathbf{D}}_e(\omega)] \cdot \tilde{\mathbf{d}}(\omega) + i\tilde{\xi}_{sc}(\omega) + i\tilde{\xi}_e(\omega). \quad (\text{C11})$$

where $\tilde{\xi}_{sc}(\omega)$, $\tilde{\xi}_e(\omega)$ are the random forces, $\tilde{\mathbf{D}}_{sc}(\omega)$, $\tilde{\mathbf{D}}_e(\omega)$ are the dissipation kernels, and they are given by

$$\begin{aligned} \tilde{\xi}_{sc}(\omega) &:= \sum_{\mathbf{k}} \mathbf{T}_{\mathbf{k}} \cdot \mathbf{G}_{sc}(\omega, \mathbf{k}) \cdot \hat{\mathbf{c}}_{\mathbf{k}}(0), \quad \tilde{\xi}_e(\omega) := \tilde{\xi}_1 + \tilde{\xi}_N := \sum_{x=1,N} \sum_{\mathbf{k}} \mathbf{Y}_{x,\mathbf{k}} \cdot \mathbf{G}_{e-x}(\omega, \mathbf{k}) \cdot \hat{\mathbf{b}}_{x,\mathbf{k}}(0), \\ \tilde{\mathbf{D}}_{sc}(\omega) &:= \sum_{\mathbf{k}} \mathbf{T}_{\mathbf{k}} \cdot \mathbf{G}_{sc}(\omega, \mathbf{k}) \cdot \mathbf{T}_{\mathbf{k}}^\dagger, \quad \tilde{\mathbf{D}}_e(\omega) := \tilde{\mathbf{D}}_{e-1} + \tilde{\mathbf{D}}_{e-N} := \sum_{x=1,N} \sum_{\mathbf{k}} \mathbf{Y}_{x,\mathbf{k}} \cdot \mathbf{G}_{e-x}(\omega, \mathbf{k}) \cdot \mathbf{Y}_{x,\mathbf{k}}^\dagger. \end{aligned} \quad (\text{C12})$$

In the time domain, Eq. (C11) gives the quantum Langevin equation in the main text

$$\partial_t \hat{\mathbf{d}} = \hat{\mathbf{d}}(0)\delta(t) - i\mathbf{H}_w \cdot \hat{\mathbf{d}}(t) - \int_0^t d\tau \mathbf{D}(t-\tau) \cdot \hat{\mathbf{d}}(\tau) + i\hat{\xi}_{sc}(t) + i\hat{\xi}_e(t), \quad (\text{C13})$$

where $\mathbf{D}(t) := \mathbf{D}_{sc}(t) + \mathbf{D}_e(t)$, and $\hat{\mathbf{d}}(0)\delta(t)$ brings in the initial condition (omitted in the main text). Then the nanowire dynamics can be obtained from the Langevin equation (C11), i.e.,

$$\tilde{\mathbf{d}}(\omega) = \mathbf{G}(\omega) \cdot [\hat{\mathbf{d}}(0) + i\tilde{\xi}_{sc}(\omega) + i\tilde{\xi}_e(\omega)], \quad \mathbf{G}(\omega) := i[\omega^+ - \mathbf{H}_w + i\tilde{\mathbf{D}}_{sc}(\omega) + i\tilde{\mathbf{D}}_e(\omega)]^{-1}, \quad (\text{C14})$$

where $[\mathbf{G}(\omega)]_{4N \times 4N}$ is the Green function for the nanowire.

APPENDIX D: THE DISSIPATION KERNEL AND EFFECTIVE INTERACTION

The dissipation kernels in Eq. (C12) provide both dissipation effect and effective interaction to the nanowire system. For the two electron leads, with the help of the Green functions (C10) and tunneling matrices (C9), the dissipation kernel $\tilde{\mathbf{D}}_e(\omega) = [\tilde{\mathbf{D}}_{e-1} + \tilde{\mathbf{D}}_{e-N}](\omega)$ is given by

$$\begin{aligned} \tilde{\mathbf{D}}_{e-1}(\omega) &= \sum_{\mathbf{k}} \mathbf{Y}_{1,\mathbf{k}} \cdot \mathbf{G}_{e-1}(\omega, \mathbf{k}) \cdot \mathbf{Y}_{1,\mathbf{k}}^\dagger = \text{diag}\{\tilde{\mathbf{D}}_{e-1}(\omega), \mathbf{0}, \dots, \mathbf{0}\}, \quad \tilde{\mathbf{D}}_{e-N} = \text{diag}\{\mathbf{0}, \dots, \mathbf{0}, \tilde{\mathbf{D}}_{e-N}\}, \\ \tilde{\mathbf{D}}_{e-x}(\omega) &:= \sum_{\mathbf{k}} \mathbf{Y}_{x,\mathbf{k}} \cdot \mathbf{G}_{e-x}(\omega, \mathbf{k}) \cdot \mathbf{Y}_{x,\mathbf{k}}^\dagger = \sum_{\mathbf{k}} |g_{x,\mathbf{k}}|^2 \text{diag}\left\{ \frac{i}{\omega^+ - \varepsilon_{x,\mathbf{k}}}, \frac{i}{\omega^+ - \varepsilon_{x,\mathbf{k}}}, \frac{i}{\omega^+ + \varepsilon_{x,\mathbf{k}}}, \frac{i}{\omega^+ + \varepsilon_{x,\mathbf{k}}} \right\}. \end{aligned} \quad (\text{D1})$$

The above summation over the electron modes \mathbf{k} can be turned into an integral by introducing $\Upsilon_x(\omega)$ as the spectral density of the coupling strength between the nanowire and lead x , i.e.,

$$\Upsilon_x(\omega) := 2\pi \sum_{\mathbf{k}} |g_{x,\mathbf{k}}|^2 \delta(\omega - \varepsilon_{x,\mathbf{k}}) \sum_{\mathbf{k}} \frac{i|g_{x,\mathbf{k}}|^2}{\omega^+ \pm \varepsilon_{x,\mathbf{k}}} \longrightarrow i \int_{-\infty}^{+\infty} \frac{d\varepsilon}{2\pi} \frac{\Upsilon_x(\varepsilon)}{\omega + i\epsilon \pm \varepsilon} = i\mathcal{P} \int \frac{d\varepsilon}{2\pi} \frac{\Upsilon_x(\varepsilon)}{\omega \pm \varepsilon} + \frac{1}{2} \Upsilon_x(\pm\omega). \quad (\text{D2})$$

The first term of the principle integral provides an energy correction to the system Hamiltonian \mathbf{H}_w in the Green function (C14), and the second term provides the dissipation effect. In transport measurements, the coupling spectral density is usually approximated as a constant $\Upsilon_x(\omega) \equiv \Upsilon_x$, which is also known as the wide band limit. Thus, the above energy correction gives zero, only left $\tilde{\mathbf{D}}_{e-x}(\omega) \simeq \frac{1}{2} \Upsilon_x \text{diag}\{1, 1, 1, 1\} := \frac{1}{2} \Upsilon_x$. As a result, the dissipation kernel of the two electron leads only

provides the dissipation effect, i.e., $\tilde{\mathbf{D}}_e(\omega) \simeq \frac{1}{2}\tilde{\Gamma}_e(\omega) := \frac{1}{2}(\Gamma_1 + \Gamma_N)$, where $\Gamma_1 := \text{diag}\{\Gamma_1, \dots, \mathbf{0}, \mathbf{0}\}$, $\Gamma_N := \text{diag}\{\mathbf{0}, \dots, \mathbf{0}, \Gamma_N\}$ are $4N \times 4N$ dissipation matrices.

Similarly, the dissipation kernel from the s -wave SC [Eq. (C12)] is treated in the same way, which gives

$$\tilde{\mathbf{D}}_{sc}(\omega) = \sum_{\mathbf{k}} \mathbf{T}_{\mathbf{k}} \cdot \mathbf{G}_{sc}(\omega, \mathbf{k}) \cdot \mathbf{T}_{\mathbf{k}}^\dagger \simeq \text{diag}\{\tilde{\mathbf{D}}_1^s(\omega), \dots, \tilde{\mathbf{D}}_N^s(\omega)\}, \quad \tilde{\mathbf{D}}_n^s(\omega) := \sum_{\mathbf{k}} \mathbf{T}_{n,\mathbf{k}} \cdot \frac{i}{\omega^+ - \mathbf{H}_{sc}(\mathbf{k})} \cdot \mathbf{T}_{n,\mathbf{k}}^\dagger \equiv \tilde{\mathbf{D}}_s(\omega). \quad (\text{D3})$$

Here the off-diagonal blocks in $[\tilde{\mathbf{D}}_{sc}(\omega)]_{4N \times 4N}$ are omitted for the local tunneling approximation, which means the tunneling processes from different sites of the nanowire to the s -wave SC do not have any interferences or correlations with each other. Besides, since the coupling strengths between different sites and the s -wave SC have the same amplitude, $|J_{m,\mathbf{k}}| = |J_{n,\mathbf{k}}| := J_{\mathbf{k}}$ for $m \neq n$, all the N diagonal blocks in $\tilde{\mathbf{D}}_{sc}(\omega)$ are equal to each other, and they are given by

$$\tilde{\mathbf{D}}_s(\omega) = \sum_{\mathbf{k}} \mathbf{T}_{\mathbf{k}} \cdot \frac{i}{\omega^+ - \mathbf{H}_{sc}(\mathbf{k})} \cdot \mathbf{T}_{\mathbf{k}}^\dagger = \sum_{\mathbf{k}} \frac{i|J_{\mathbf{k}}|^2}{(\omega^+)^2 - (\epsilon_{\mathbf{k}}^{sc})^2 - \Delta_s^2} \begin{bmatrix} \omega^+ + \epsilon_{\mathbf{k}}^{sc} & & & -\Delta_s \\ & \omega^+ + \epsilon_{\mathbf{k}}^{sc} & \Delta_s & \\ & \Delta_s & \omega^+ - \epsilon_{\mathbf{k}}^{sc} & \\ -\Delta_s & & & \omega^+ - \epsilon_{\mathbf{k}}^{sc} \end{bmatrix},$$

$$\frac{1}{(\omega^+)^2 - E^2} = \frac{1}{2E} \left[\frac{1}{\omega^+ - E} - \frac{1}{\omega^+ + E} \right] = \frac{1}{2E} \left[\mathcal{P} \frac{1}{\omega - E} - i\pi \delta(\omega - E) - \mathcal{P} \frac{1}{\omega + E} + i\pi \delta(\omega + E) \right], \quad (\text{D4})$$

where $\mathbf{T}_{\mathbf{k}} := |J_{\mathbf{k}}| \text{diag}\{1, 1, -1, -1\}$. Similarly like Eq. (D2), the summation over \mathbf{k} can be turned into an integral by introducing $\Upsilon_s(\omega)$ as the the spectral density of the coupling strength between the nanowire and the s -wave SC, i.e.,

$$\Upsilon_s(\omega) := \pi \sum_{\mathbf{k}} |J_{\mathbf{k}}|^2 \delta(\omega - \epsilon_{\mathbf{k}}^{sc}) \sim \pi |J_s(\omega)|^2 \rho_s(\omega). \quad (\text{D5})$$

Here $\rho_s(\omega)$ is the density of state from the s -wave SC, and approximately $\Upsilon_s(\omega) \simeq \Upsilon_s$ is a constant. Then the dissipation kernel $\tilde{\mathbf{D}}_s(\omega)$ from the s -wave SC is obtained as

$$\tilde{\mathbf{D}}_s(\omega) = \frac{1}{2}\tilde{\Gamma}_s^+(\omega) + i\tilde{\mathbf{V}}_s(\omega) := \frac{1}{2}[\tilde{\Gamma}_s^+(\omega) + \tilde{\Gamma}_s^-(\omega)] + i\tilde{\mathbf{V}}_s(\omega), \quad \tilde{\mathbf{V}}_s(\omega) = -\frac{\Theta(\Delta_s - |\omega|)\Upsilon_s}{\sqrt{\Delta_s^2 - \omega^2}} \begin{bmatrix} \omega & & & -\Delta_s \\ & \omega & \Delta_s & \\ & \Delta_s & \omega & \\ -\Delta_s & & & \omega \end{bmatrix},$$

$$\tilde{\Gamma}_s^\pm(\omega) = \pm \frac{2\Theta(\pm\omega - \Delta)\Upsilon_s}{\sqrt{\omega^2 - \Delta^2}} \begin{bmatrix} \omega & & & -\Delta_s \\ & \omega & \Delta_s & \\ & \Delta_s & \omega & \\ -\Delta_s & & & \omega \end{bmatrix}, \quad (\text{D6})$$

where $\tilde{\Gamma}_s(\omega)$ indicates the dissipation effect, while $\tilde{\mathbf{V}}_s(\omega)$ can be regarded as an effective interaction in the Green function (C14). Correspondingly, the full dissipation kernel (D3) can be written as $\tilde{\mathbf{D}}_{sc}(\omega) := \frac{1}{2}\tilde{\Gamma}_s(\omega) + i\tilde{\mathbf{V}}_s(\omega)$, with $\tilde{\mathbf{V}}_s(\omega) := \text{diag}\{\tilde{\mathbf{V}}_s, \dots, \tilde{\mathbf{V}}_s\}$ and $\tilde{\Gamma}_s(\omega) := \text{diag}\{\tilde{\Gamma}_s, \dots, \tilde{\Gamma}_s\}$.

It is worth noticing that the Heaviside function appears in both $\tilde{\Gamma}_s(\omega)$ and $\tilde{\mathbf{V}}_s(\omega)$. That means, when the system energy lies within the SC gap $|\omega| < \Delta_s$, the s -wave SC only provides the effective pairing (the SC proximity) without any dissipation effect; for the high energy modes outside the SC gap $|\omega| > \Delta_s$, the s -wave SC only gives the dissipation effect but does not induce the SC proximity.

APPENDIX E: STEADY STATE CURRENT

Here we consider the electric current flowing from lead 1 to the nanowire, and the differential conductance measurement. Generally, the electric current can be calculated by the changing rate of the electron number in lead 1, that is,

$$\langle \hat{I}_1(t) \rangle = -e \sum_{\mathbf{k}_s} \partial_t \langle \hat{b}_{1,\mathbf{k}_s}^\dagger \hat{b}_{1,\mathbf{k}_s} \rangle = \frac{ie}{\hbar} \sum_{\mathbf{k}_s} [\mathbf{g}_{1,\mathbf{k}} \langle \hat{d}_{1s}^\dagger(t) \hat{b}_{1,\mathbf{k}_s}(t) \rangle - \mathbf{g}_{1,\mathbf{k}}^* \langle \hat{b}_{1,\mathbf{k}_s}^\dagger(t) \hat{d}_{1s}(t) \rangle] := I_1(t) + \text{c.c.} \quad (\text{E1})$$

In particular, we focus on the steady state current after a long enough time relaxation $t \rightarrow \infty$. This can be obtained from the Fourier image $\tilde{I}_1(\omega)$ based on the *final value theorem*, which gives $I_1(t \rightarrow +\infty) = \lim_{\omega \rightarrow 0} [-i\omega \tilde{I}_1(\omega)]$. With the help of the tunneling matrix $\mathbf{Y}_{1,\mathbf{k}}$ and a projector operator \mathbf{P}^+ defined below, $\tilde{I}_1(\omega)$ can be rewritten as the following

matrix form:

$$\begin{aligned}
\tilde{I}_1(\omega) &= \frac{ie}{\hbar} \sum_{\mathbf{k}} \int \frac{d\nu}{2\pi} \langle [\tilde{\mathbf{d}}(\nu)]^\dagger \cdot \mathbf{P}^+ \cdot \mathbf{Y}_{1,\mathbf{k}} \cdot \tilde{\mathbf{b}}_{1,\mathbf{k}}(\nu + \omega) \rangle \\
&= \frac{ie}{\hbar} \int d\nu \langle [-i\tilde{\xi}_{\text{sc}}^\dagger(\nu) - i\tilde{\xi}_e^\dagger(\nu)] \cdot \mathbf{G}^\dagger(\nu) \cdot \mathbf{P}^+ \cdot [\tilde{\xi}_1(\nu + \omega) + i\tilde{\mathbf{D}}_{e-1}(\nu + \omega) \cdot \tilde{\mathbf{d}}(\nu + \omega)] \rangle \\
&= \frac{e}{\hbar} \int d\nu \langle \{[\tilde{\xi}_{\text{sc}}^\dagger + \tilde{\xi}_1^\dagger + \tilde{\xi}_N^\dagger] \cdot \mathbf{G}^\dagger\}_{(\nu)} \cdot \mathbf{P}^+ \cdot \{\tilde{\xi}_1 - \tilde{\mathbf{D}}_{e-1} \cdot \mathbf{G} \cdot [\tilde{\xi}_{\text{sc}} + \tilde{\xi}_1 + \tilde{\xi}_N]\}_{(\nu+\omega)} \rangle.
\end{aligned} \tag{E2}$$

Here the projector \mathbf{P}^+ is defined as $\mathbf{P}^+ := \text{diag}\{\mathbf{P}^+, \mathbf{P}^+, \dots, \mathbf{P}^+\}$, with blocks $\mathbf{P}^+ := \text{diag}\{1, 1, 0, 0\}$. The dynamics of $\tilde{\mathbf{b}}_{1,\mathbf{k}}(\nu + \omega)$, $[\tilde{\mathbf{d}}(\nu)]^\dagger$ has been given in Eqs. (C10) and (C14), and the initial states of the nanowire like $\tilde{\mathbf{d}}(0)$ do not appear here since their contributions would decay to zero in the steady state $t \rightarrow \infty$.

The quantum expectations in Eq. (E2) are calculated from the random forces $\tilde{\xi}_{\text{sc}}$, $\tilde{\xi}_e$ based on the initial states of lead 1, N and the s -wave SC, and they can be expressed by the correlation matrices for these three fermionic baths, $[\mathbb{C}_1(\bar{\omega}, \omega)]_{mn} := \langle [\tilde{\xi}_1^\dagger(\bar{\omega})]_n [\tilde{\xi}_1(\omega)]_m \rangle$, $[\mathbb{C}_s(\bar{\omega}, \omega)]_{mn} := \langle [\tilde{\xi}_{\text{sc}}^\dagger(\bar{\omega})]_n [\tilde{\xi}_{\text{sc}}(\omega)]_m \rangle$, which further give

$$\begin{aligned}
\tilde{I}_1(\omega) &= \frac{e}{\hbar} \int d\nu \text{tr}[\mathbb{C}_1(\nu, \omega + \nu) \cdot \mathbf{G}^\dagger(\nu) \cdot \mathbf{P}^+] - \sum_{y=1,N} \text{tr}[\mathbb{C}_y(\nu, \omega + \nu) \cdot \mathbf{G}^\dagger(\nu) \cdot \mathbf{P}^+ \cdot \tilde{\mathbf{D}}_{e-1}(\nu + \omega) \cdot \mathbf{G}(\nu + \omega)] \\
&\quad - \text{tr}[\mathbb{C}_s(\nu, \omega + \nu) \cdot \mathbf{G}^\dagger(\nu) \cdot \mathbf{P}^+ \cdot \tilde{\mathbf{D}}_{e-x}(\nu + \omega) \cdot \mathbf{G}(\nu + \omega)].
\end{aligned} \tag{E3}$$

According to the final value theorem, with the help of the correlation matrices $\mathbb{C}_{x,s}(\bar{\omega}, \omega)$ calculated in Appendix F, in the steady state $t \rightarrow \infty$, the electric current is obtained as [40]

$$\begin{aligned}
\langle \hat{I}_1 \rangle_\infty &= \frac{e}{\hbar} \int d\nu \text{tr}[\mathbf{G}^\dagger \Gamma_1^+ \mathbf{G} \Gamma_N^+]_{(\nu)} [f_1(\nu) - f_N(\nu)] + \text{tr}[\mathbf{G}^\dagger \Gamma_1^+ \mathbf{G} \Gamma_N^-]_{(\nu)} [f_1(\nu) - \bar{f}_N(-\nu)] \\
&\quad + \text{tr}[\mathbf{G}^\dagger \Gamma_1^+ \mathbf{G} \Gamma_1^-]_{(\nu)} [f_1(\nu) - \bar{f}_1(-\nu)] + \text{tr}[\mathbf{G}^\dagger \Gamma_1^+ \mathbf{G} \tilde{\Gamma}_s]_{(\nu)} f_1(\nu) - \text{tr}[\mathbf{G}^\dagger \Gamma_1^+ \mathbf{G} \tilde{\Gamma}_s^+]_{(\nu)} f_s(\nu) - \text{tr}[\mathbf{G}^\dagger \Gamma_1^+ \mathbf{G} \tilde{\Gamma}_s^-]_{(\nu)} \bar{f}_s(-\nu).
\end{aligned} \tag{E4}$$

Here the dot symbols for the matrix product “ \cdot ” are omitted for short. $f_x(\nu)$, $f_s(\nu)$ are the Fermi distributions of lead x and the s -wave SC, and $\bar{f}_{x,s}(\omega) := 1 - f_{x,s}(\omega)$. The dissipation matrices $\tilde{\Gamma}_s(\nu)$, Γ_x have been given in Eqs. (D1), (D2), and (D6). Γ_x^\pm and $\tilde{\Gamma}_s^\pm(\nu)$ are dissipation matrices of lead x and the s -wave SC, which are given in Eqs. (F4) and (F7). The following relation is needed when deriving the above result:

$$\mathbf{G} + \mathbf{G}^\dagger = \mathbf{G}^\dagger \cdot [i(\omega - \mathbf{H} - i\tilde{\mathbf{D}}) - i(\omega - \mathbf{H} + i\tilde{\mathbf{D}})] \cdot \mathbf{G} = \mathbf{G}^\dagger \cdot (\Gamma_1 + \Gamma_N + \tilde{\Gamma}_s) \cdot \mathbf{G}. \tag{E5}$$

For a transport measurement, we set the chemical potentials as $\mu_N = 0$, $\mu_1 = eV$, with V as the voltage bias. At the zero temperature, the chemical potential of lead 1 is $f_1(\nu) = \Theta(eV - \nu)$, thus the above electric current (E4) gives the differential conductance $\sigma \equiv dI_1/dV$ as

$$\sigma = \frac{e^2}{\hbar} \{ \text{tr}[\mathbf{G}^\dagger \Gamma_1^+ \mathbf{G} \Gamma_N]_{(eV)} + \text{tr}[\mathbf{G}^\dagger \Gamma_1^+ \mathbf{G} \tilde{\Gamma}_s]_{(eV)} + \text{tr}[\mathbf{G}^\dagger \Gamma_1^+ \mathbf{G} \Gamma_1^-]_{(eV)} + \text{tr}[\mathbf{G}^\dagger \Gamma_1^+ \mathbf{G} \Gamma_1^-]_{(-eV)} \}. \tag{E6}$$

The first two terms indicate the contributions from the electron exchange from lead 1 to lead N and the s -wave SC. The last two terms come from the Andreev reflection between lead 1 and the nanowire. In the above derivations, except the local tunneling approximation and the constant coupling spectrum, no other approximations are made. Thus, in principle this result also applies for the situations when the magnetic field or coupling strength is strong.

APPENDIX F: CORRELATION MATRICES OF THE BATHS

Here we calculate the correlation matrices in the above current (E3). From the random force (C12), Green function (C10), and the tunneling matrix (C9), the $4N \times 4N$ correlation matrix $[\mathbb{C}_x(\bar{\omega}, \omega)]_{mn} := \langle [\tilde{\xi}_x^\dagger(\bar{\omega})]_n [\tilde{\xi}_x(\omega)]_m \rangle$ for lead x is

$$\begin{aligned}
\mathbb{C}_1(\bar{\omega}, \omega) &= \text{diag}\{\mathbb{C}_1(\bar{\omega}, \omega), \mathbf{0}, \dots, \mathbf{0}\}, \quad \mathbb{C}_N(\bar{\omega}, \omega) = \text{diag}\{\mathbf{0}, \dots, \mathbf{0}, \mathbb{C}_N(\bar{\omega}, \omega)\}, \\
[\mathbb{C}_x(\bar{\omega}, \omega)]_{4 \times 4} &= \sum_{\mathbf{k}} \text{diag} \left\{ \frac{|\mathbf{g}_{x,\mathbf{k}}|^2 f_x(\varepsilon_{\mathbf{k}})}{(\bar{\omega}^- - \varepsilon_{\mathbf{k}})(\omega^+ - \varepsilon_{\mathbf{k}})}, \frac{|\mathbf{g}_{x,\mathbf{k}}|^2 f_x(\varepsilon_{\mathbf{k}})}{(\bar{\omega}^- - \varepsilon_{\mathbf{k}})(\omega^+ - \varepsilon_{\mathbf{k}})}, \frac{|\mathbf{g}_{x,\mathbf{k}}|^2 \bar{f}_x(\varepsilon_{\mathbf{k}})}{(\bar{\omega}^- + \varepsilon_{\mathbf{k}})(\omega^+ + \varepsilon_{\mathbf{k}})}, \frac{|\mathbf{g}_{x,\mathbf{k}}|^2 \bar{f}_x(\varepsilon_{\mathbf{k}})}{(\bar{\omega}^- + \varepsilon_{\mathbf{k}})(\omega^+ + \varepsilon_{\mathbf{k}})} \right\} \\
&= \text{diag} \left\{ \frac{i\Upsilon_x(\omega) f_x(\omega)}{(\omega - \bar{\omega}) + 2i\epsilon}, \frac{i\Upsilon_x(\omega) f_x(\omega)}{(\omega - \bar{\omega}) + 2i\epsilon}, \frac{i\Upsilon_x(-\bar{\omega}) \bar{f}_x(-\bar{\omega})}{(\omega - \bar{\omega}) + 2i\epsilon}, \frac{i\Upsilon_x(-\bar{\omega}) \bar{f}_x(-\bar{\omega})}{(\omega - \bar{\omega}) + 2i\epsilon} \right\}.
\end{aligned} \tag{F1}$$

Here $f_x(\omega)$ is the Fermi distribution from the initial equilibrium state of lead x , i.e.,

$$f_x(\omega) = \langle \hat{b}_{x,\mathbf{k}}^\dagger(0) \hat{b}_{x,\mathbf{k}}(0) \rangle = \frac{1}{e^{(\omega - \mu_x)/T_x} + 1} \xrightarrow{T_x \rightarrow 0} \Theta(\mu_x - \omega), \quad \bar{f}_x(\omega) := 1 - f_x(\omega). \tag{F2}$$

The above summations of \mathbf{k} are turned into integrals by using the coupling spectral density $\Upsilon_x(\omega) \equiv \Upsilon_x$, i.e.,

$$\begin{aligned} \sum_{\mathbf{k}} \frac{|g_{x,\mathbf{k}}|^2 f_x(\varepsilon_{\mathbf{k}})}{(\bar{\omega}^- - \varepsilon_{\mathbf{k}})(\omega^+ - \varepsilon_{\mathbf{k}})} &\rightarrow \int \frac{d\nu}{2\pi} \frac{\Upsilon_x(\nu) f_x(\nu)}{(\nu - \bar{\omega} + i\epsilon)(\nu - \omega - i\epsilon)} = \frac{i\Upsilon_x(\omega) f_x(\omega)}{(\omega - \bar{\omega}) + 2i\epsilon}, \\ \sum_{\mathbf{k}} \frac{|g_x(\mathbf{k})|^2 \bar{f}_x(\varepsilon_{\mathbf{k}})}{(\bar{\omega}^- + \varepsilon_{\mathbf{k}})(\omega^+ + \varepsilon_{\mathbf{k}})} &\rightarrow \int \frac{d\nu}{2\pi} \frac{\Upsilon_x(\nu) \bar{f}_x(\nu)}{(\nu + \bar{\omega} - i\epsilon)(\nu + \omega + i\epsilon)} = \frac{i\Upsilon_x(-\bar{\omega}) \bar{f}_x(-\bar{\omega})}{(\omega - \bar{\omega}) + 2i\epsilon}. \end{aligned} \quad (\text{F3})$$

Therefore, when calculating the steady state current from the final value theorem, the correlation matrix in Eq. (E3) gives

$$\begin{aligned} \lim_{\omega \rightarrow 0} [(-i\omega) \mathbf{C}_x(\nu, \omega + \nu)] &= \Upsilon_x \text{diag}\{f_x(\nu), f_x(\nu), \bar{f}_x(-\nu), \bar{f}_x(-\nu)\} := f_x(\nu) \Gamma_x^+ + \bar{f}_x(-\nu) \Gamma_x^-, \\ \lim_{\omega \rightarrow 0} [(-i\omega) \mathbf{C}_x(\nu, \omega + \nu)] &= f_x(\nu) \Gamma_x^+ + \bar{f}_x(-\nu) \Gamma_x^-, \end{aligned} \quad (\text{F4})$$

where $\Gamma_x^+ := \Upsilon_x \text{diag}\{1, 1, 0, 0\}$ and $\Gamma_x^- := \Upsilon_x \text{diag}\{0, 0, 1, 1\}$ are upper and lower parts of the dissipation matrix $\Gamma_x \equiv \Gamma_x^+ + \Gamma_x^-$, respectively, and correspondingly $\Gamma_1^\pm := \text{diag}\{\Gamma_1^\pm, \mathbf{0}, \dots, \mathbf{0}\}$, $\Gamma_N^\pm := \text{diag}\{\mathbf{0}, \dots, \mathbf{0}, \Gamma_N^\pm\}$.

On the other hand, to calculate the correlation matrix for the s -wave SC, we need to use the Bogoliubov eigenmodes, which determine the initial Fermi distribution of the s -wave SC. The s -wave SC Hamiltonian is diagonalized as $\hat{H}_{\text{sc}} = \frac{1}{2} \sum_{\mathbf{k}} \hat{\mathbf{c}}_{\mathbf{k}}^\dagger \cdot \mathbf{H}_{\mathbf{k}}^{\text{sc}} \cdot \hat{\mathbf{c}}_{\mathbf{k}} \equiv \frac{1}{2} \sum_{\mathbf{k}} \hat{\eta}_{\mathbf{k}}^\dagger \cdot \mathbf{E}_{\mathbf{k}}^{\text{sc}} \cdot \hat{\eta}_{\mathbf{k}}$, with $\hat{\eta}_{\mathbf{k}} := \mathbf{U}_{\mathbf{k}} \cdot \hat{\mathbf{c}}_{\mathbf{k}}$ and

$$\mathbf{E}_{\mathbf{k}}^{\text{sc}} := \begin{bmatrix} E_{\mathbf{k}}^{\text{sc}} & & & \\ & E_{\mathbf{k}}^{\text{sc}} & & \\ & & -E_{\mathbf{k}}^{\text{sc}} & \\ & & & -E_{\mathbf{k}}^{\text{sc}} \end{bmatrix} = \mathbf{U}_{\mathbf{k}} \cdot \mathbf{H}_{\mathbf{k}}^{\text{sc}} \cdot \mathbf{U}_{\mathbf{k}}^\dagger, \quad \mathbf{U}_{\mathbf{k}} = \begin{bmatrix} \cos \theta_{\mathbf{k}} & & & \sin \theta_{\mathbf{k}} \\ & \cos \theta_{\mathbf{k}} & -\sin \theta_{\mathbf{k}} & \\ & \sin \theta_{\mathbf{k}} & \cos \theta_{\mathbf{k}} & \\ -\sin \theta_{\mathbf{k}} & & & \cos \theta_{\mathbf{k}} \end{bmatrix}, \quad (\text{F5})$$

where $E_{\mathbf{k}}^{\text{sc}} \equiv [(\epsilon_{\mathbf{k}}^{\text{sc}})^2 + \Delta_s^2]^{1/2}$ and $\tan 2\theta_{\mathbf{k}} \equiv \Delta_s / \epsilon_{\mathbf{k}}^{\text{sc}}$ [see also Eq. (A6)].

From the random force (C12), the correlation matrix of the s -wave SC gives $[\mathbf{C}_s(\bar{\omega}, \omega)]_{mn} := \langle [\tilde{\xi}_{\text{sc}}^\dagger(\bar{\omega})]_n [\tilde{\xi}_{\text{sc}}(\omega)]_m \rangle \simeq \text{diag}\{\mathbf{C}_s(\bar{\omega}, \omega), \dots, \mathbf{C}_s(\bar{\omega}, \omega)\}$, which is block diagonal. Similarly, as the treatment to the dissipation kernel (D3), the off-diagonal blocks are omitted for the local tunneling approximation. And the diagonal blocks $\mathbf{C}_s(\bar{\omega}, \omega)$ are calculated as

$$\begin{aligned} [\mathbf{C}_s(\bar{\omega}, \omega)]_{mn} &= \sum_{\mathbf{k}, i, j} \langle [\hat{\mathbf{c}}_{\mathbf{k}}^\dagger(0)]_i [\mathbf{G}_{\text{sc}}^\dagger(\bar{\omega}) \mathbf{T}_{\mathbf{k}}^\dagger]_{in} \cdot [\mathbf{T}_{\mathbf{k}} \mathbf{G}_{\text{sc}}(\omega)]_{mj} [\hat{\mathbf{c}}_{\mathbf{k}}(0)]_j \rangle \\ &= \sum_{\mathbf{k}} \mathbf{T}_{\mathbf{k}} \cdot \mathbf{G}_{\text{sc}}(\omega) \cdot [\mathbf{1} - \langle \hat{\mathbf{c}}_{\mathbf{k}}(0) \hat{\mathbf{c}}_{\mathbf{k}}^\dagger(0) \rangle] \cdot \mathbf{G}_{\text{sc}}^\dagger(\bar{\omega}) \cdot \mathbf{T}_{\mathbf{k}}^\dagger = \sum_{\mathbf{k}} \mathbf{T}_{\mathbf{k}} \cdot \mathbf{G}_{\text{sc}}(\omega) \cdot \mathbf{U}_{\mathbf{k}}^\dagger \cdot [\mathbf{1} - \langle \hat{\eta}_{\mathbf{k}}(0) \hat{\eta}_{\mathbf{k}}^\dagger(0) \rangle] \cdot \mathbf{U}_{\mathbf{k}} \cdot \mathbf{G}_{\text{sc}}^\dagger(\bar{\omega}) \cdot \mathbf{T}_{\mathbf{k}}^\dagger \\ &= \sum_{\mathbf{k}} \mathbf{T}_{\mathbf{k}} \cdot \mathbf{U}_{\mathbf{k}}^\dagger \cdot \frac{i}{\omega^+ - \mathbf{E}_{\mathbf{k}}^{\text{sc}}} \cdot \text{diag}\{f_s(E_{\mathbf{k}}^{\text{sc}}), f_s(E_{\mathbf{k}}^{\text{sc}}), \bar{f}_s(E_{\mathbf{k}}^{\text{sc}}), \bar{f}_s(E_{\mathbf{k}}^{\text{sc}})\} \cdot \frac{-i}{\bar{\omega}^- - \mathbf{E}_{\mathbf{k}}^{\text{sc}}} \cdot \mathbf{U}_{\mathbf{k}} \cdot \mathbf{T}_{\mathbf{k}}^\dagger \\ &= \sum_{\mathbf{k}} \frac{|J_{\mathbf{k}}|^2 f_s(E_{\mathbf{k}}^{\text{sc}})/2}{(\omega^+ - E_{\mathbf{k}}^{\text{sc}})(\bar{\omega}^- - E_{\mathbf{k}}^{\text{sc}})} \begin{bmatrix} 1 + \cos 2\theta_{\mathbf{k}} & & & -\sin 2\theta_{\mathbf{k}} \\ & 1 + \cos 2\theta_{\mathbf{k}} & \sin 2\theta_{\mathbf{k}} & \\ & \sin 2\theta_{\mathbf{k}} & 1 - \cos 2\theta_{\mathbf{k}} & \\ -\sin 2\theta_{\mathbf{k}} & & & 1 - \cos 2\theta_{\mathbf{k}} \end{bmatrix} \\ &+ \frac{|J_{\mathbf{k}}|^2 \bar{f}_s(E_{\mathbf{k}}^{\text{sc}})/2}{(\omega^+ + E_{\mathbf{k}}^{\text{sc}})(\bar{\omega}^- + E_{\mathbf{k}}^{\text{sc}})} \begin{bmatrix} 1 - \cos 2\theta_{\mathbf{k}} & & & \sin 2\theta_{\mathbf{k}} \\ & 1 - \cos 2\theta_{\mathbf{k}} & -\sin 2\theta_{\mathbf{k}} & \\ & -\sin 2\theta_{\mathbf{k}} & 1 + \cos 2\theta_{\mathbf{k}} & \\ \sin 2\theta_{\mathbf{k}} & & & 1 + \cos 2\theta_{\mathbf{k}} \end{bmatrix}, \end{aligned} \quad (\text{F6})$$

where $f_s(E_{\mathbf{k}}^{\text{sc}})$ is the Fermi distribution for the Bogoliubov eigenmodes in the initial state. The summation over the fermion modes \mathbf{k} can be turned into an integral with the help of the coupling spectral density $\Upsilon_s(\omega) \equiv \Upsilon_s$. Furthermore, when calculating the steady state current from the final value theorem, the correlation matrix $\mathbf{C}_s(\bar{\omega}, \omega)$ gives

$$\begin{aligned} \lim_{\omega \rightarrow 0} [(-i\omega) \mathbf{C}_s(\nu, \omega + \nu)] &= \frac{2\Upsilon_s}{\sqrt{\nu^2 - \Delta_s^2}} [\Theta(\nu - \Delta_s) f_s(\nu) - \Theta(-\Delta_s - \nu) \bar{f}_s(-\nu)] \begin{bmatrix} \nu & & & -\Delta_s \\ & \nu & \Delta_s & \\ & \Delta_s & \nu & \\ -\Delta_s & & & \nu \end{bmatrix} \\ &= f_s(\nu) \tilde{\Gamma}_s^+(\nu) + \bar{f}_s(-\nu) \tilde{\Gamma}_s^-(\nu), \quad \lim_{\omega \rightarrow 0} [(-i\omega) \mathbf{C}_s(\nu, \omega + \nu)] := f_s(\nu) \tilde{\Gamma}_s^+(\nu) + \bar{f}_s(-\nu) \tilde{\Gamma}_s^-(\nu), \end{aligned} \quad (\text{F7})$$

where $\tilde{\Gamma}_s^\pm(\nu) := \text{diag}\{\tilde{\Gamma}_s^\pm(\nu), \tilde{\Gamma}_s^\pm(\nu), \dots, \tilde{\Gamma}_s^\pm(\nu)\}$. To obtain this result, the following derivation is adopted [$\mathcal{F}(x)$ is an arbitrary function]:

$$\begin{aligned} & \lim_{\bar{\omega} \rightarrow \omega} \left[-i(\omega - \bar{\omega}) \int_{-\infty}^{\infty} \frac{d\varepsilon}{2\pi} \frac{\mathcal{F}(\sqrt{\varepsilon^2 + \Delta_s^2})}{(\omega^+ \pm \sqrt{\varepsilon^2 + \Delta_s^2})(\bar{\omega}^- \pm \sqrt{\varepsilon^2 + \Delta_s^2})} \right] \\ &= \lim_{\bar{\omega} \rightarrow \omega} \int_{-\infty}^{\infty} \frac{d\varepsilon}{2\pi} i(\bar{\omega}^- - \omega^+) \left[\frac{1}{\omega^+ \pm \sqrt{\varepsilon^2 + \Delta_s^2}} - \frac{1}{\bar{\omega}^- \pm \sqrt{\varepsilon^2 + \Delta_s^2}} \right] \frac{\mathcal{F}(\sqrt{\varepsilon^2 + \Delta_s^2})}{\bar{\omega}^- - \omega^+} \\ &= \int_{-\infty}^{\infty} d\varepsilon \mathcal{F}(\sqrt{\varepsilon^2 + \Delta_s^2}) \delta(\omega \pm \sqrt{\varepsilon^2 + \Delta_s^2}) = 2 \int_0^{\infty} dE \frac{E \mathcal{F}(E) \delta(\omega \pm E)}{\sqrt{E^2 - \Delta_s^2}} = \mp \frac{\Theta(\mp\omega - \Delta_s)}{\sqrt{\omega^2 - \Delta_s^2}} \cdot 2\omega \mathcal{F}(\mp\omega). \quad (\text{F8}) \end{aligned}$$

-
- [1] A. Y. Kitaev, *Phys. Usp.* **44**, 131 (2001).
[2] J. D. Sau, R. M. Lutchyn, S. Tewari, and S. Das Sarma, *Phys. Rev. Lett.* **104**, 040502 (2010).
[3] J. Alicea, *Rep. Prog. Phys.* **75**, 076501 (2012).
[4] R. M. Lutchyn, E. P. A. M. Bakkers, L. P. Kouwenhoven, P. Krogstrup, C. M. Marcus, and Y. Oreg, *Nat. Rev. Mater.* **3**, 52 (2018).
[5] C. Reeg and D. L. Maslov, *Phys. Rev. B* **95**, 205439 (2017).
[6] T. D. Stanescu and S. Das Sarma, *Phys. Rev. B* **96**, 014510 (2017).
[7] C.-X. Liu, J. D. Sau, T. D. Stanescu, and S. Das Sarma, *Phys. Rev. B* **96**, 075161 (2017).
[8] A. Y. Kitaev, *Ann. Phys.* **303**, 2 (2003).
[9] C. Nayak, S. H. Simon, A. Stern, M. Freedman, and S. Das Sarma, *Rev. Mod. Phys.* **80**, 1083 (2008).
[10] V. Mourik, K. Zuo, S. M. Frolov, S. R. Plissard, E. P. A. M. Bakkers, and L. P. Kouwenhoven, *Science* **336**, 1003 (2012).
[11] A. Das, Y. Ronen, Y. Most, Y. Oreg, M. Heiblum, and H. Shtrikman, *Nat. Phys.* **8**, 887 (2012).
[12] K. T. Law, P. A. Lee, and T. K. Ng, *Phys. Rev. Lett.* **103**, 237001 (2009).
[13] K. Flensberg, *Phys. Rev. B* **82**, 180516(R) (2010).
[14] D. Chevallier and J. Klinovaja, *Phys. Rev. B* **94**, 035417 (2016).
[15] F. Nichele, A. C. C. Drachmann, A. M. Whiticar, E. C. T. O'Farrell, H. J. Suominen, A. Fornieri, T. Wang, G. C. Gardner, C. Thomas, A. T. Hatke, P. Krogstrup, M. J. Manfra, K. Flensberg, and C. M. Marcus, *Phys. Rev. Lett.* **119**, 136803 (2017).
[16] D. Liu, G. Zhang, Z. Cao, H. Zhang, and D. E. Liu, *Phys. Rev. Lett.* **128**, 076802 (2022).
[17] X.-J. Liu, *Phys. Rev. Lett.* **109**, 106404 (2012).
[18] M. T. Deng, S. Vaitiekėnas, E. B. Hansen, J. Danon, M. Leijnse, K. Flensberg, J. Nygård, P. Krogstrup, and C. M. Marcus, *Science* **354**, 1557 (2016).
[19] O. Millo and G. Koren, *Philos. Trans. R. Soc. London Sect. A* **376**, 20140143 (2018).
[20] S. Sasaki, S. De Franceschi, J. M. Elzerman, W. G. van der Wiel, M. Eto, S. Tarucha, and L. P. Kouwenhoven, *Nature (London)* **405**, 764 (2000).
[21] E. J. H. Lee, X. Jiang, R. Aguado, G. Katsaros, C. M. Lieber, and S. De Franceschi, *Phys. Rev. Lett.* **109**, 186802 (2012).
[22] L. Fu and C. L. Kane, *Phys. Rev. Lett.* **100**, 096407 (2008).
[23] Y. Oreg, G. Refael, and F. von Oppen, *Phys. Rev. Lett.* **105**, 177002 (2010).
[24] J. Alicea, *Phys. Rev. B* **81**, 125318 (2010).
[25] J. D. Sau, S. Tewari, R. M. Lutchyn, T. D. Stanescu, and S. Das Sarma, *Phys. Rev. B* **82**, 214509 (2010).
[26] E. M. Stoudenmire, J. Alicea, O. A. Starykh, and M. P. A. Fisher, *Phys. Rev. B* **84**, 014503 (2011).
[27] T. D. Stanescu, J. D. Sau, R. M. Lutchyn, and S. Das Sarma, *Phys. Rev. B* **81**, 241310(R) (2010).
[28] J. D. Sau, R. M. Lutchyn, S. Tewari, and S. Das Sarma, *Phys. Rev. B* **82**, 094522 (2010).
[29] A. C. Potter and P. A. Lee, *Phys. Rev. B* **83**, 184520 (2011).
[30] Y. Peng, F. Pientka, L. I. Glazman, and F. von Oppen, *Phys. Rev. Lett.* **114**, 106801 (2015).
[31] C. Reeg, D. Loss, and J. Klinovaja, *Phys. Rev. B* **96**, 125426 (2017).
[32] Y. Asano and Y. Tanaka, *Phys. Rev. B* **87**, 104513 (2013).
[33] H. Fröhlich, *Phys. Rev.* **79**, 845 (1950).
[34] S. Nakajima, *Adv. Phys.* **4**, 363 (1955).
[35] J. R. Schrieffer and P. A. Wolff, *Phys. Rev.* **149**, 491 (1966).
[36] A. Dhar and B. S. Shastry, *Phys. Rev. B* **67**, 195405 (2003).
[37] A. Dhar and D. Roy, *J. Stat. Phys.* **125**, 801 (2006).
[38] D. Roy, C. J. Bolech, and N. Shah, *Phys. Rev. B* **86**, 094503 (2012).
[39] L.-P. Yang, C. Y. Cai, D. Z. Xu, W.-M. Zhang, and C. P. Sun, *Phys. Rev. A* **87**, 012110 (2013).
[40] S.-W. Li, Z.-Z. Li, C. Y. Cai, and C. P. Sun, *Phys. Rev. B* **89**, 134505 (2014).
[41] P. Ghosh, J. D. Sau, S. Tewari, and S. Das Sarma, *Phys. Rev. B* **82**, 184525 (2010).
[42] B. van Heck, R. M. Lutchyn, and L. I. Glazman, *Phys. Rev. B* **93**, 235431 (2016).
[43] N. A. Court, A. J. Ferguson, and R. G. Clark, *Supercond. Sci. Technol.* **21**, 015013 (2008).
[44] A. C. Potter and P. A. Lee, *Phys. Rev. B* **83**, 094525 (2011).
[45] J. Liu, A. C. Potter, K. T. Law, and P. A. Lee, *Phys. Rev. Lett.* **109**, 267002 (2012).
[46] S. Gangadharaiah, B. Braunecker, P. Simon, and D. Loss, *Phys. Rev. Lett.* **107**, 036801 (2011).
[47] E. Sela, A. Altland, and A. Rosch, *Phys. Rev. B* **84**, 085114 (2011).
[48] T. D. Stanescu, R. M. Lutchyn, and S. Das Sarma, *Phys. Rev. B* **84**, 144522 (2011).

- [49] H. Zhang, C.-X. Liu, S. Gazibegovic, D. Xu, J. A. Logan, G. Wang, N. van Loo, J. D. S. Bommer, M. W. A. de Moor, D. Car, R. L. M. Op het Veld, P. J. van Veldhoven, S. Koelling, M. A. Verheijen, M. Pendharkar, D. J. Pennachio, B. Shojaei, J. S. Lee, C. J. Palmstrøm, E. P. A. M. Bakkers *et al.*, [Nature \(London\)](#) **556**, 74 (2018).
- [50] S. Nadj-Perge, V. S. Pribiag, J. W. G. van den Berg, K. Zuo, S. R. Plissard, E. P. A. M. Bakkers, S. M. Frolov, and L. P. Kouwenhoven, [Phys. Rev. Lett.](#) **108**, 166801 (2012).
- [51] T. Hong, K. Choi, K. Ik Sim, T. Ha, B. Cheol Park, H. Yamamori, and J. Hoon Kim, [J. Appl. Phys.](#) **114**, 243905 (2013).